THE JOURNAL OF COMPARATIVE NEUROLOGY 241:111-137 (1985)

Synaptic Connections of Intracellularly Filled Clutch Cells: A Type of Small Basket Cell in the Visual Cortex of the Cat

Z.F. KISVÁRDAY, K.A.C. MARTIN, D. WHITTERIDGE, AND P. SOMOGYI
Department of Experimental Psychology, Oxford University, Oxford OX1 3UD, United Kingdom (Z.F.K., K.A.C.M., D.W.), 1st Department of Anatomy, Semmelweis Medical School, 1450, Budapest, IX, Tüzoltó u 58, Hungary (Z.F.K., P.S.), and Department of Human Physiology, Flinders Medical Centre, Bedford Park, South Australia 5042 (P.S.)

ABSTRACT

Light and electron microscopic quantitative analysis was carried out on a type of neuron intracellularly filled with horseradish peroxidase. Two cells were studied in area 17, one of which was injected intra-axonally, and its soma was not recovered. One cell was studied in area 18. The two somata were on the border of layers IVa/b; they were radially elongated and received synapses from numerous large boutons with round synaptic vesicles. The dendrites were smooth and remained largely in layer IV.

The cells can be recognised on the basis of their axonal arbor, which was restricted to layer IV (90–95% of boutons) with minor projections to layers III, V, and VI. Many of the large, bulbous boutons contacted neuronal somata, short collaterals often forming "claw"-like configurations around cells. The name "clutch cell" is suggested to delineate this type of neuron from other aspiny multipolar cells. Computer-assisted reconstruction of the axon showed that in layer IV the axons occupied a rectangular area about 300 × 500 μm, elongated anteroposteriorly in area 17 and mediolaterally in area 18. The distributions of synaptic boutons and postsynaptic cells were patchy within this area. A total of 321 boutons were serially sectioned in area 17. The boutons formed type II synaptic contacts. The postsynaptic targets were somata (20–30%), dendritic shafts (35–50%), spines (30%), and rarely axon initial segments. Most of the postsynaptic somata tested were not immunoreactive for GABA and their fine structural features suggest that they are spiny stellate, star pyramidal, and pyramidal neurons. The characteristics of most of the postsynaptic dendrites and spines also suggest that they belong to these spiny neurons. A few of the postsynaptic dendrites and somata exhibited characteristics of cells with smooth dendrites and these somata were immunoreactive for GABA.

It is suggested that clutch cells are inhibitory interneurons exerting their effect mainly on layer IV spiny neurons in an area localised perhaps to a single ocular dominance column. The specific laminar location of the axons of clutch cell also suggests that they may be associated with the afferent terminals of lateral geniculate nucleus cells, and could thus be responsible for generating some of the selective properties of neurons of the first stage of cortical processing.

Key words: interneurons, three-dimensional reconstruction, cortical inhibition, GABA, light and electron microscopy

One important role of the visual cortex is to transform the sensory data arriving from the retina via subcortical nuclei into the process of perception. In the cat, the first stage of this transformation occurs at the first cortical synapse: the nonoriented centre-surround fields of the retina

Accepted June 24, 1985.

P. Somogyi's present address is MRC Anatomical Neuropharmacology Unit, University Department of Pharmacology, South Parks Road, Oxford OX1 3QT, U.K.

and the lateral geniculate nucleus (LGN) are transformed into fields that are selective for properties such as orientation, direction of movement, and length and width of the stimuli (Hubel and Wiesel, '62). Only a very small minority of cells in layer IV have receptive fields that are comparable to those of LGN cells (Hubel and Wiesel, '62). The mechanisms by which this remarkable transformation takes place remain speculative. Evidence is gradually accumulating, however, which indicates that many of these emergent properties may be generated by intracortical inhibition (Hubel and Wiesel, '62; Bishop et al., '71; Blakemore and Tobin, '72; Benevento et al., '72; Creutzfeldt et al., '74; Morrone et al., '82; Heggelund and Moors, '83). This inhibition also appears to be mediated by characteristic types of GABA-ergic interneurones (Sillito, '75, '77, '79; Tsumoto et al., '79).

Physiological studies (Hoffman and Stone, '71; Henry et al., '79; Bullier and Henry, '79; Ferster and Lindström, '83; Martin and Whitteridge, '84) indicate that the vast majority of neurons in layer IV receive a monosynaptic input from the LGN afferents and that their receptive field properties show the selectivity characteristic of cortical cells. Of the different neuronal types in layer IV, the spiny stellate and pyramidal types are thought to be excitatory in nature (see Emson and Lindvall, '79; Lund, '84). By contrast, many of the cells with smooth or sparsely spiny dendrites are immunoreactive for GABA-ergic markers, implying that they are probably responsible for the inhibitory mechanisms (Ribak, '78; Somogyi et al., '83a,b; Somogyi and Hodgson, '85). If this assumption is correct, then clearly an understanding of the synaptic organisation of the cells with smooth dendrites is a necessary step in our investigation of the first stage of cortical processing.

We have identified one particular cell type for study: a multipolar neurone with smooth dendrites that is particularly associated with layer IV. The cells studied were injected intracellularly with HRP and thus we can be reasonably sure that the axonal ramifications were complete. Our light microscopic studies indicated that the dense axonal plexus was confined largely to layer IV, and that many of the boutons contacted the somata of other layer IV neurons (Martin et al., '83). Since the soma is considered an ideal site for inhibition (Eccles, '64; Jack et al., '75) and since most boutons on the soma in layer IV are immunoreactive for glutamate decarboxylase (GAD) (Freund et al., '83), the enzyme synthesizing GABA, it was suggested that these layer IV multipolar cells were inhibitory interneurons (Martin et al., '83). The specific association of the cell's axon with the geniculocortical termination zone suggests that this small multipolar cell may play a role in generating specific receptive field properties at the first stage of cortical processing. Therefore the present study was undertaken (1) to determine the spatial distribution and numerical parameters of the axons of these cells and their postsynaptic targets; (2) to characterise the structural features and synaptic input of the cells; and (3) to determine the postsynaptic targets and their neurochemical characteristics. Preliminary reports of some of the findings have been published (Kisvárday et al., '83; Martin et al., '83).

MATERIALS AND METHODS

Animals, surgery, and electrophysiology

Material was obtained from three of 57 adult cats used in physiological experiments (Martin and Whitteridge, '84), which were carried out to study the structural features of physiologically characterised neurons in the visual cortex. The cats were anaesthetised with a mixture of Fluothane/N_2O/O_2, paralysed with gallamine triethiodide and tubocurarine, and maintained under Althesin (Glaxo) or barbiturate anaesthesia. Blood pressure, heart rate, end tidal CO_2 and temperature were monitored continuously. Surgical, electrical stimulation, and recording conditions have been described in detail elsewhere (Martin and Whitteridge, '84). Neurons were recorded from both extra- and intracellularly by using glass micropipettes filled with 4% horseradish peroxidase (HRP, Boehringer, grade 1) in 0.2 M KCl and 0.05 M Tris at pH 7.9. After establishing the position and properties of the receptive field and latency to electrical stimulation, the neurons were filled iontophoretically with HRP.

Fixation and tissue processing

At the termination of recording, the cats were given an overdose of anaesthetic and were perfused through the heart with saline followed by a fixative containing 2.5% glutaraldehyde and 1% paraformaldehyde in 0.1 M phosphate buffer (PB). Since several neurons were filled in each animal, between 2 and 20 hours elapsed between filling a neurone and fixation. A block of cortex was cut out from the brain and sectioned in the coronal plane, at 80 μm, using a Vibratome (Oxford Instruments). The sections were washed extensively with 0.1 M PB and reacted for HRP enzyme activity using the *p*-phenylenediamine/pyrocatechol procedure (Hanker et al., '77) with cobalt/nickel intensification (Adams, '81; Perry and Linden, '82). After further washing the sections were treated with 1% OsO_4, dissolved in 0.1 M PB, dehydrated, and mounted on slides in Durcupan ACM resin (Fluka). To enhance contrast for electron microscopy 1% uranyl acetate was included in the 70% ethanol.

Light microscopy and three-dimensional reconstruction

The neurones were drawn with the aid of a 50× oil immersion objective and a drawing tube. The individual drawings obtained from single sections were superimposed to obtain a two-dimensional image of the cells (Figs. 1A, 3A, 6). The cells were also recorded on series of light micrographs.

In order to analyse the three-dimensional structure of the axonal arborisation and the distribution of the boutons, a complete three-dimensional reconstruction was made of neuron 1. We used a PDP 11/34 computer and a Quantimet image analyser system equipped with a microscope fitted with drawing tube and stepping motors that positioned the stage with 0.5 μm accuracy in the X, Y, and Z dimensions. The whole axon and the position of each bouton and branch point were recorded by using a 50× oil immersion objective and the software NEURON, NEUMER, NEUROT, and NRN11A and statistical programs (as set up at Dept. of Anatomy, Semmelweis Medical School; see also Zsuppan, '84). All measurements refer to values as seen in the sections.

One of the conspicuous features of these multipolar cells is that their axonal boutons surround the somata of other neurones. As proved by subsequent electron microscopy these latter neurones are the postsynaptic targets of clutch cells and their position outlines the area influenced by the

multipolar cells. Therefore we recorded the X, Y, and Z coordinates of each presumed postsynaptic neuron, as represented by its nucleolus, by using the same software as for the boutons. Layering of the cortex followed previous studies (O'Leary '41; Lund et al., '79).

Electron microscopy and quantitative analysis of dendrites

Areas of interest were reembedded from the slides for correlated electron microscopy (Somogyi et al., '79). Serial ultrathin sections were mounted on Formvar-coated single-slot grids and stained with lead citrate. Several hundreds of serial sections from the dense axon plexus of both cell 1 and 2 were analysed to obtain a representative sample of postsynaptic elements. Each HRP-filled bouton in the plane of the section was photographed at the synaptic junction and the postsynaptic structure was identified, if necessary by following it in the series. The sampled area represented the whole width of the axon arborization and both layers IVA and IVB.

In addition, a selected sample of identified collaterals, especially those surrounding cell bodies, were analysed for postsynaptic targets and for subsequent postembedding GABA immunocytochemistry of the postsynaptic neurones. The parent cell type of dendritic profiles in electron micrographs are difficult to identify. Therefore we used the area of the dendritic profiles, the area occupied by mitochondria, and the length of plasma membrane occupied by synaptic junctions for their characterisation. Data were obtained by an electronic planimeter and values refer to dimensions in the sections. All measurements were taken at the plane where the HRP-filled clutch cell boutons formed a synaptic junction. The sample of postsynaptic dendrites seen in this study were compared with the sample of postsynaptic dendrites contacted by the large basket cells examined in an earlier publication (Somogyi et al., '83b).

Immunocytochemistry

Postsynaptic somata were heterogeneous with regard to their fine structural features. To see if this could be correlated with neurochemical hetrogeneity, we tested some of them using postembedding GABA immunocytochemistry as described earlier (Somogyi et al., '85). First the synaptic contact was confirmed by electron microscopy between the HRP-filled boutons and the neuronal somata; then two or three 0.5-μm thick sections were cut from that part of the somata which was still in the block. These sections were incubated on glass slides to reveal GABA immunoreactivity. An antiserum to GABA (code No. 7, Hodgson et al., '85) was used at a dilution of 1:2,000 in the unlabeled antibody enzyme method (Sternberger et al., '70). The same reagents and conditions were used as earlier (Somogyi et al., '85).

RESULTS

Definition of clutch cells

The name "clutch cell" is suggested to distinguish the neurones illustrated in this study from the wide range of 'multipolar' cells (Peters and Regidor, '81; Meyer, '83). The characteristic feature of the cell is its large bulbous boutons apposed to neural somata, and a circumscribed axonal field that is restricted mainly to layer IV (Figs. 9A, 10A, 13A, 16A–C). Bouton-laden short axon collaterals of clutch cells often form "claw"-like configurations around the postsynaptic cells. Although the pattern of termination of clutch cells on somata is similar to that of large basket cells (Martin et al., '83; Somogyi et al., '83b) and of a basket cell in superficial layers (De Felipe and Fairén, '82), the laminar distribution of the boutons of the two basket cell types is distinctly different. Further properties of the clutch cells will be discussed following the presentation of the results.

TABLE 1. Location of Clutch Cells Analysed in This Study

Cell No.	Cat. No.	Area	Position in visual field: Azimuth	Position in visual field: Elevation	Position of cell body
CC1	23/81	17	0.0°	−11.4°	Border of IVa/IVb
CC2	22/82	17	2.9°	−2.6°	Axon only
CC3	24/83	18	2.9°	−3.2°	Border of IVa/IVb

Neurones analysed

The three cells were similar on the basis of their axonal morphology and the position of their boutons around neuronal somata (Table 1). Cell No. 1 (CC1) was in area 17; its physiological properties and a preliminary description of its light microscopic features have been published (Martin et al., '83). It was then called a "multipolar cell." It had overlapping on and off subfields (C-type receptive field) and responded optimally to bars shorter than the receptive field length. It was driven monosynaptically by Y-type afferents from the contralateral eye.

Cell No. 2 (CC2) was injected in its main axon and was also in area 17. The HRP did not fill the cell body and the dendrites of this neuron, but it strongly filled the axon to the tips of the terminal branches. In addition, a pyramidal cell in layer III, whose basal dendrite descended into layer IV and passed by the injected axon, was also injected in this penetration. Consequently the physiological data obtained while recording the single unit cannot be attributed to either of the two individual cells. Such "double" fillings, making up about 10% of our overall sample, are not uncommon in intracellular marking studies and many explanations have been proposed (see Methods, Martin and Whitteridge, '84). Even in the absence of physiological data the structural features were of sufficient interest for further analysis.

Cell No. 3 (CC3) was in area 18, and it was also a "double" with an accompanying spiny stellate cell. This meant that no physiological data could be attributed to this neuron. Because of the very different axonal and dendritic pattern of the two neurons, they could easily be separated during reconstruction. It is worth noting that both the units recorded during the filling of CC2 and CC3 were monosynaptically activated by Y-type afferents and had non-overlapping on and off subfields (S-type receptive fields).

Structural features detected by light microscopy

The position of the three cells studied is shown in Table 1. The cell bodies of CC1 in area 17 and CC3 in area 18 were in layer IV. Both somata were elongated radially, 25–30 μm long and about 15 μm wide (Figs. 1A, 6, 7A, 15A). Most of the dendrites originated from thick dendritic stems at the lower and upper poles of the cells. The thick stems divided into numerous secondary dendrites which rarely branched subsequently. Most of the dendrites remained

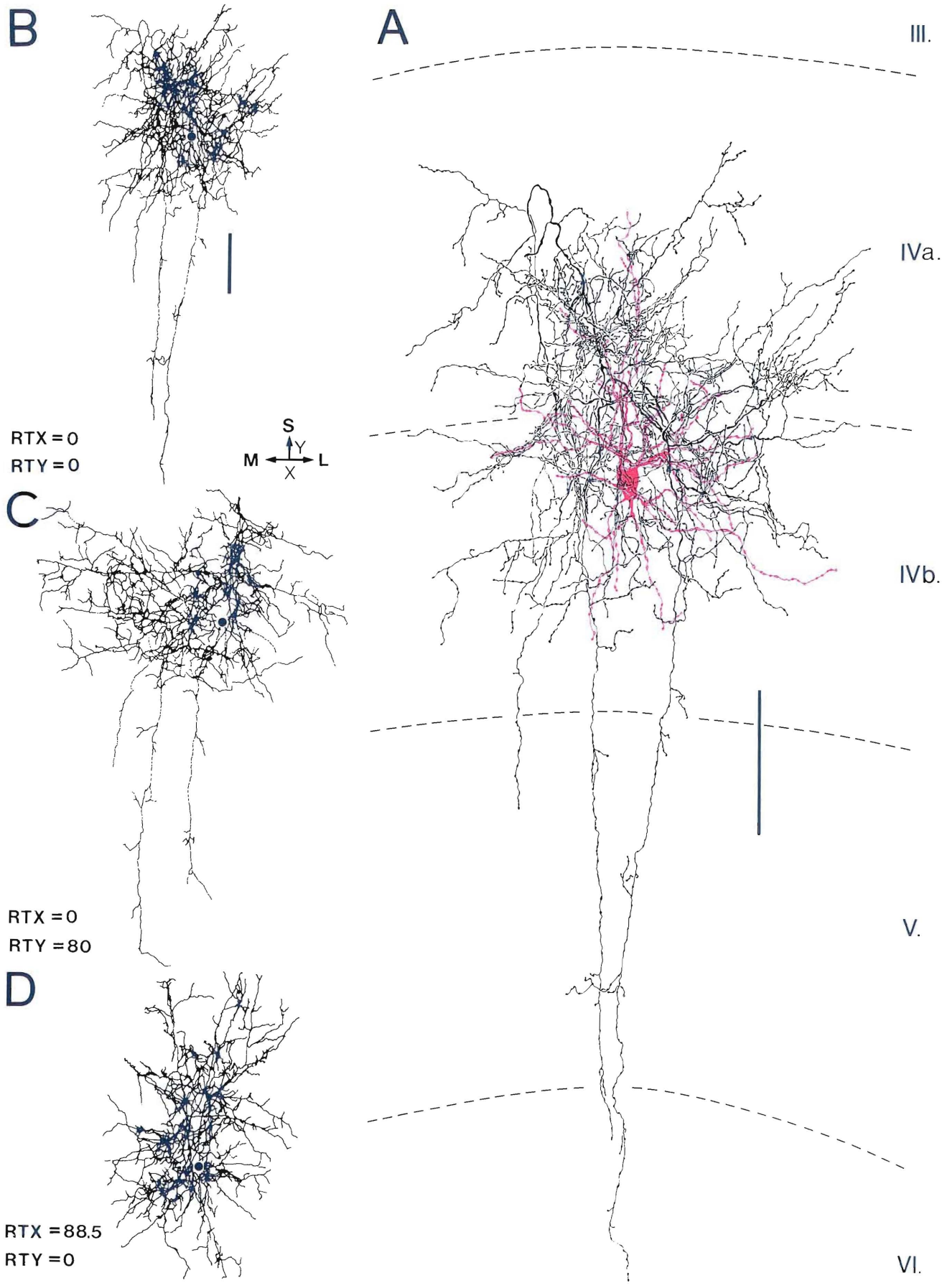

Figure 1

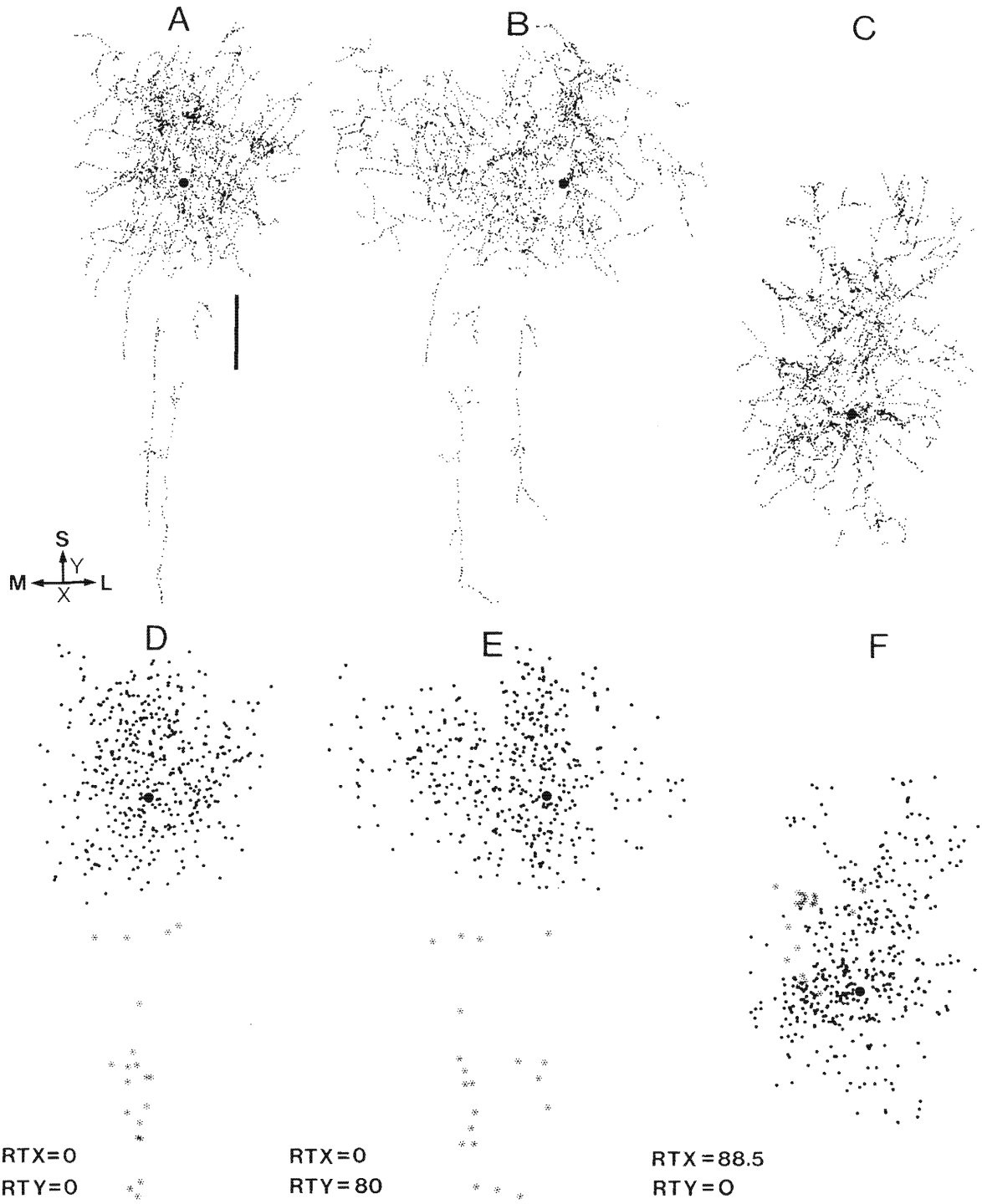

Fig. 2. A–C. Distribution of synaptic boutons on the axon of clutch cell No. 1 in the same three planes as in Figure 1. Although the dots represent axonal boutons traced from the light microscope, subsequent electron microscopy showed that the boutons made synaptic contacts. D–F. Distribution of neuronal somata in layers IV (dots) and V–VI (asterisks) contacted by boutons of clutch cell 1. Electron microscopy on a sample showed that most boutons contacting somata established synaptic contacts with them. The synaptic boutons and postsynaptic somata are unevenly distributed within the axon arborisation. L, lateral; M, medial; S, superior; X,Y, axes of rotation (RT). Scale = 100 μm.

Fig. 1. A. Drawing of clutch cell No. 1 in the striate cortex, from a view close to the frontal plane. Dendrites are shown in red and the axon in black. The cell was situated in a position corresponding to the cortical representation of the vertical meridian in the visual field, and received monosynaptic Y-type input. The most characteristic features are the position of the axon located largely in layer IV and the large bulbous boutons, densely placed on the axon collaterals. B. Computer reconstruction of the axon in the same plane. C. Computer rotation of the axon as viewed from the medial surface in a plane close to the sagittal plane. D. Computer rotation of the axon as viewed from the pia in a plane perpendicular to the apical dendrites. L, lateral; M, medial; S, superior; X,Y, axes of rotation (RT). Scales = 100 μm.

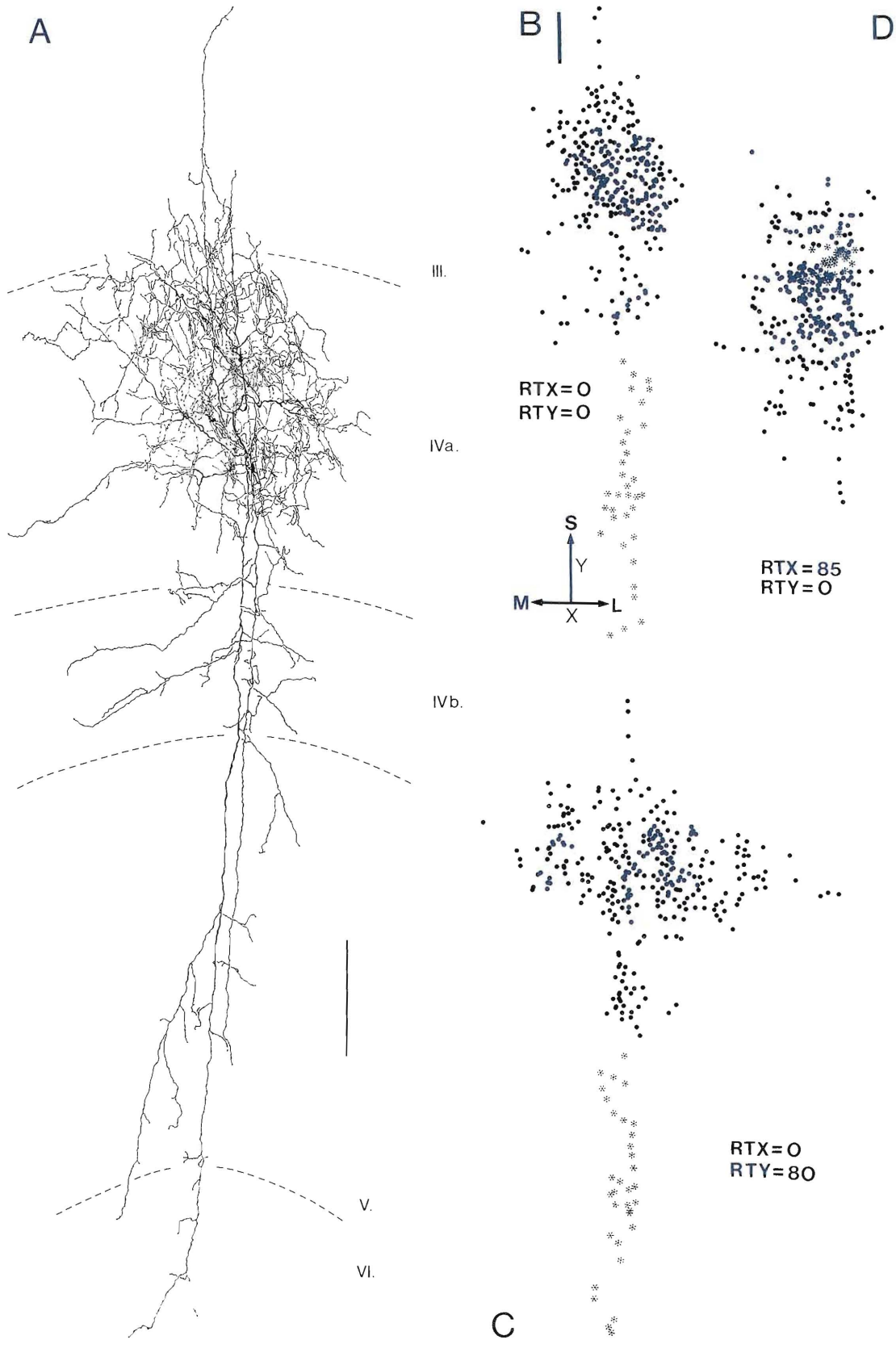

Fig. 3. A. Drawing of the axon of clutch cell No. 2, which was injected with a pyramidal neuron in the striate cortex. The distribution of synaptic boutons is very similar to that of cell 1. The apparent extension of the axon into layer III was a result of bulging of the cortex along the electrode penetration. B–D. Positions of somata contacted by boutons of the axon in layer IV (dots) and in layers V–VI (asterisks), as seen in the three principal planes. L, lateral; M, medial; S, superior; X,Y, axes of rotation (RT). Scales = 100 μm.

within layer IV. The dendrites of CC1 were strongly beaded (Figs. 1A,9D), which may in part be due to the HRP filling.

The axon of clutch cells was used for their characterization. Only the axon of CC2 was recovered but it was similar to the axon of CC1 so they will be described together. The lateral spread of both axons was 300–330 μm and they were very compact; few branches deviated from the main arbor (Figs. 1A, B, 3A). Most of the axon of CC1 was in the middle of layer IV while CC2 was mainly in IVa. The cortex was slightly bulging at the electrode penetration of CC2, which resulted in a distortion of supragranular cortical laminae. Nevertheless it could clearly be established that a few branches of this cell penetrated into lower layer III (Figs. 3A, 13C). Both axons gave numerous collaterals in layer IVb, and had two descending branches terminating in layer V and upper layer VI (Figs. 1A, 3A, 14A). Three-dimensional reconstruction and rotation of the axon arbors revealed that in the anteroposterior direction they extended to about 500 μm (Fig. 1C,D). Thus, as viewed from the pia the axons occupied a rectangular area in layer IV elongated in the anteroposterior direction. In the top view (Fig. 1D) clustering of the collaterals with an approximately 100 μm spacing could be observed.

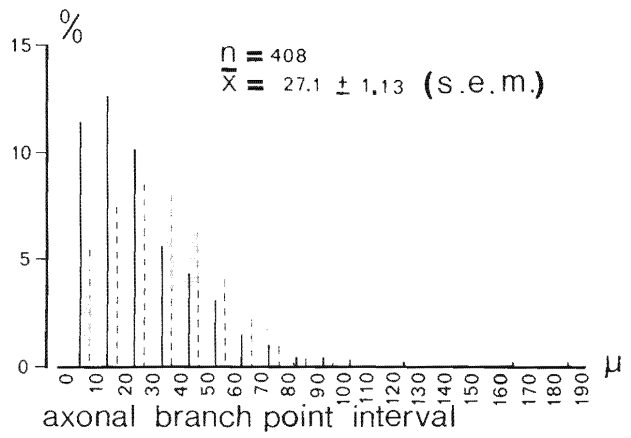

Fig. 4. Frequency distribution of branching point distances (solid lines) along the axon of clutch cell No. 1. The frequent branching of the axon produces a skewed distribution different from a normal distribution (dashed lines).

The axon of CC3 in area 18 spread in the lower part of layer IV to about 500 μm laterally (Fig. 6) and about 300 μm anteroposteriorly. The area occupied by it was thus elongated in the mediolateral direction but was very similar in size to the axons of area 17. This axon also had a descending collateral to layer V (Fig. 6).

The main axon collaterals of all three cells were smooth and about 1–2 μm thick. From the appearance of Ranvier nodes it was predicted that they had myelin sheaths. They branched very frequently at every Ranvier node, and also branched again after leaving the myelin, often giving off twiglike processes (Figs. 1, 3A, 6, 9A, 13A). The branching frequency of an axon is a conspicuous feature and therefore, for future comparison with other cell types, the branching frequency profile was compiled for the best-characterised cell (CC1; Fig. 4). The distribution is positively skewed, due to a predominance of short intervals, and differs considerably from the normal statistical distribution of a hypothetical population of the same size and having the same mean value (dotted lines, Fig. 4).

All the unmyelinated parts of the axon were studded with varicosities (Figs. 1A, 2A–C, 3A, 6, 9A, 10A, 13A, 14A, 16). Subsequent examination showed that most varicosities that were studied electron microscopically formed synaptic specializations and therefore can be considered as synaptic boutons. A comparison of Figures 1B–D with 2A–C show that only the relatively few main myelinated branches did not have boutons. Thus, the distribution of the axon branches in all three main dimensions accurately reflects the distribution of boutons, and therefore the area influenced by the cells. For future comparison of clutch cells with other neurons, we recorded the interbouton interval

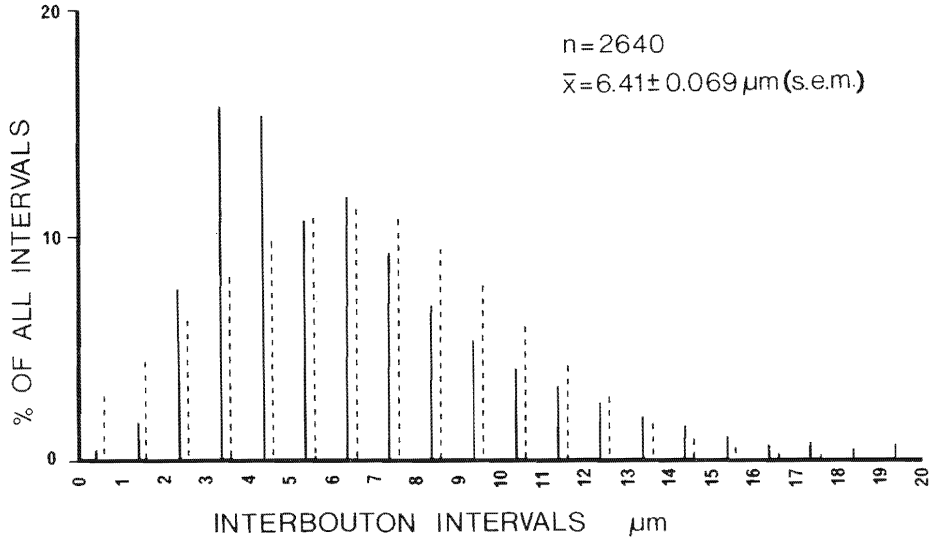

Fig. 5. Frequency distribution of interbouton intervals (solid lines) along the axon collaterals of clutch cell No. 1. Intervals longer than 20 μm and consisting of 8% of the population were not included because they are mostly myelinated main axon branches. Boutons are frequently very close to each other and this makes the distribution different from a normal distribution (dashed lines).

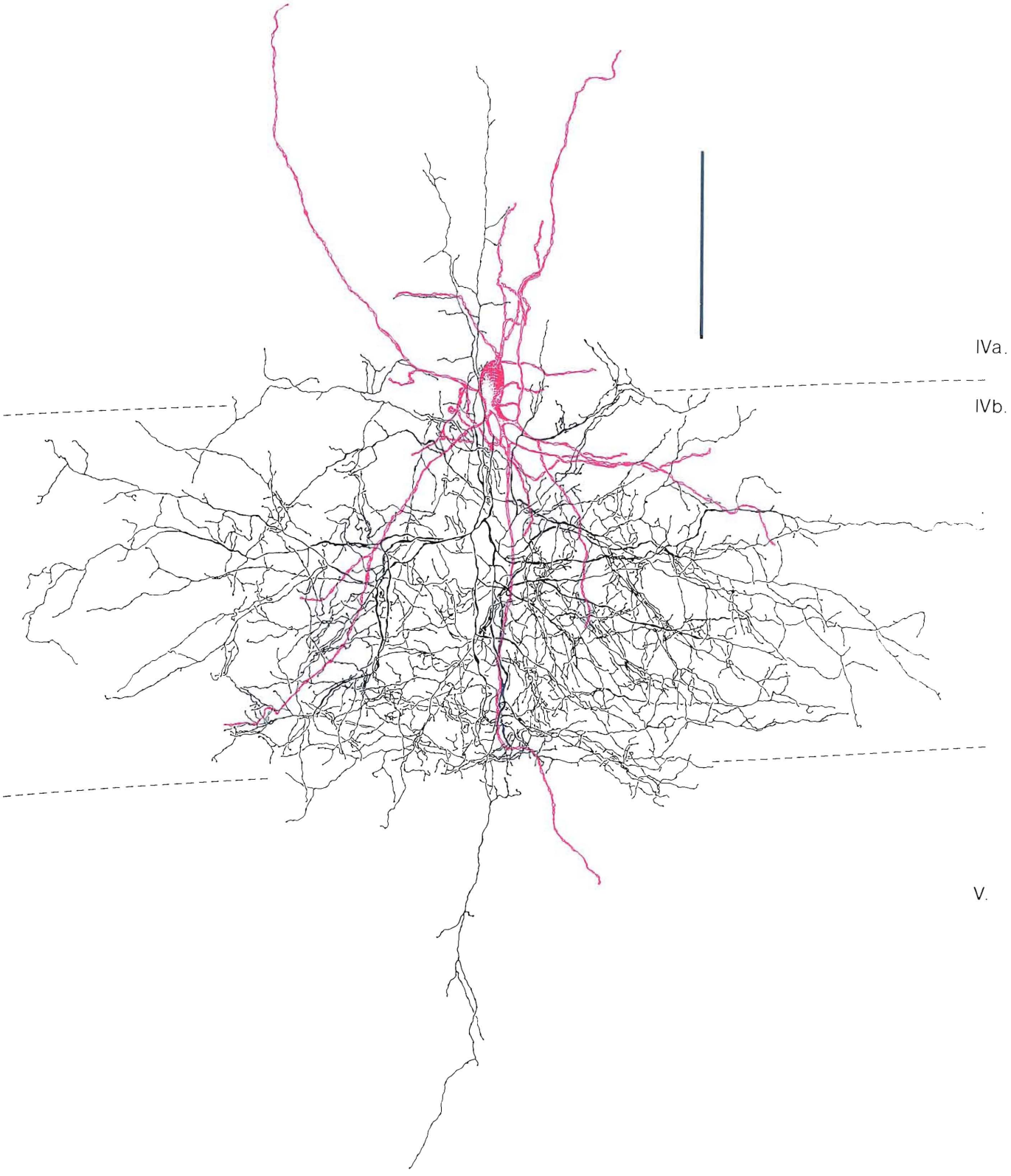

Fig. 6. Drawing of clutch cell No. 3. in the prestriate cortex, area 18. The somata and the dendrites are shown in red and the axon is shown in black. Note the concentration of boutons in lower layer IV and the abrupt decrease in the number of boutons at the layer IV/V border. Scale = 100 μm.

TABLE 2. Number of Synaptic Boutons and Synaptic Contacts From a Random Sample of Clutch Cell Axons

No. of cell	Layers examined	No. of boutons examined in the electron microscope		Total No. of postsynaptic elements		No. of postsynaptic elements in synaptic contact with a single bouton					
						1	2	3	4	Mean	
CC1	IV	147	190	184	234	113	32	1	1	1.25	1.21
	V	43		50		36	7	—	—	1.16	
CC2	IV	79		99		62	15	1	1	1.25	
CC3	IV	4		4		4	—	—	—	—	
Total		273		337							

TABLE 3. Light Microscopic Estimation of the Number of Boutons and Postsynaptic Neurons That Received Perikaryal Input From Clutch Cells 1 and 2

Cell No.	No. of boutons		No. of neural somata contacted by boutons (%)		
	Layer IV	Layers V–VI	Total	In layer IV	In layer V–VI
CC1					
On soma	1,083	20	454	434 (96)	20 (4)
Neuropil	1,650	123			
Total (%)	2,733 (95.0)	143 (5.0)	345	311 (90)	34 (10)
CC2	—	—			

profile of CC1 (Fig. 5) on the total 22,900-μm length of the axon. Short interbouton intervals predominated, giving a positively skewed distribution (compared with equivalent normal distribution, Fig. 5).

The number of boutons on the axon of clutch cell 1 is shown in Table 3. The overwhelming majority are in layer IV. From light microscopic examination 38% of the boutons contacted the soma of other neurons (Table 3, Figs. 9A, 10A). The axons of the other two cells were qualitatively very similar (Figs. 13A, 14A,B, 17A–C) but their boutons were not counted. To establish how reliable our light microscopic estimate was, 29 somata that were in apparent contact with one to five boutons of CC1 were marked randomly on light micrographs of layer IV. Correlated light and electron microscopic examination showed that the somata always received synapses from at least some of the boutons. Not all boutons could be shown to make a synaptic junction because if the section was too tangential the HRP reaction endproduct obscured the fine structural features of the junctions. Nevertheless the fact that each of the 29 somata received at least one synapse allowed us to estimate the spatial distribution and the lower limit of the number of neurones assumed to receive synapses from clutch cells 1 and 2 (Table 3).

The great majority (90–96%) of postsynaptic somata were in layer IV (Figs. 2D,E, 3B,C). Computer rotation revealed that the distribution of postsynaptic somata closely followed the distribution of clutch cell boutons (Fig. 2A–F). The top view of the position of somata receiving contacts exhibited the same rectangular shape as that of the bouton distribution, elongated in the anteroposterior direction (Figs. 2F, 3D). This shows that the different parts of the axon arborisation have a similar synaptic distribution.

Electron microscopic analysis

Soma and dendrites. The neurone examined in area 17 (CC1) was very strongly filled and the HRP leaked around the soma (Fig. 7B). The nucleus was eccentrically located, being closer to the lower pole of the cell. The cell had a high cytoplasm-to-nucleus ratio. In spite of the dense reaction endproduct and metal deposit, all the usual cytoplasmic organelles could be recognised. The cell contained numerous mitochondria, but no unique structural feature was evident (Fig. 7). More conspicuous was the neuron's synaptic input: throughout its surface the soma was densely covered by large synaptic boutons 1–3 μm in diameter and densely packed with round synaptic vesicles (Fig. 7B,C). When the synaptic contact was cut perpendicularly to the membranes, the extensive postsynaptic densities became apparent because they were not penetrated by the HRP reaction endproduct (Fig. 7D). The dendrites of this neuron were beaded and it was apparent that this was a result of swelling, seen as empty spaces on electron micrographs (Fig. 9E). The dendritic beads contained clusters of mitochondria. A high proportion of the dendritic surface was covered by synaptic contacts (Figs. 9E, 19), mainly from boutons containing round vesicles. These boutons were smaller in size than those on the somata.

The preservation of the brain from which CC3 was obtained was poor. In addition there was some oedema around the cell. Nevertheless the structural features were very similar to those of CC1 in that the soma had a high cytoplasm-to-nucleus ratio, it had an eccentric nucleus, and it received synaptic input from large boutons establishing type I contacts (Figs. 15B,C).

Axon and synaptic boutons. The main axon trunk beyond the axon initial segment and the primary axon collaterals of all three cells were covered with myelin (Figs. 9B,C, 13B, 15D). The myelin sheath was especially thick on the main axons of the two cells in area 17, becoming thinner on the smaller collaterals. The thinner tertiary and higher-order branches connecting axonal boutons were unmyelinated.

The synaptic boutons were 1–2 μm in diameter, connected by very thin axons, which gave the axon a beaded, neck-

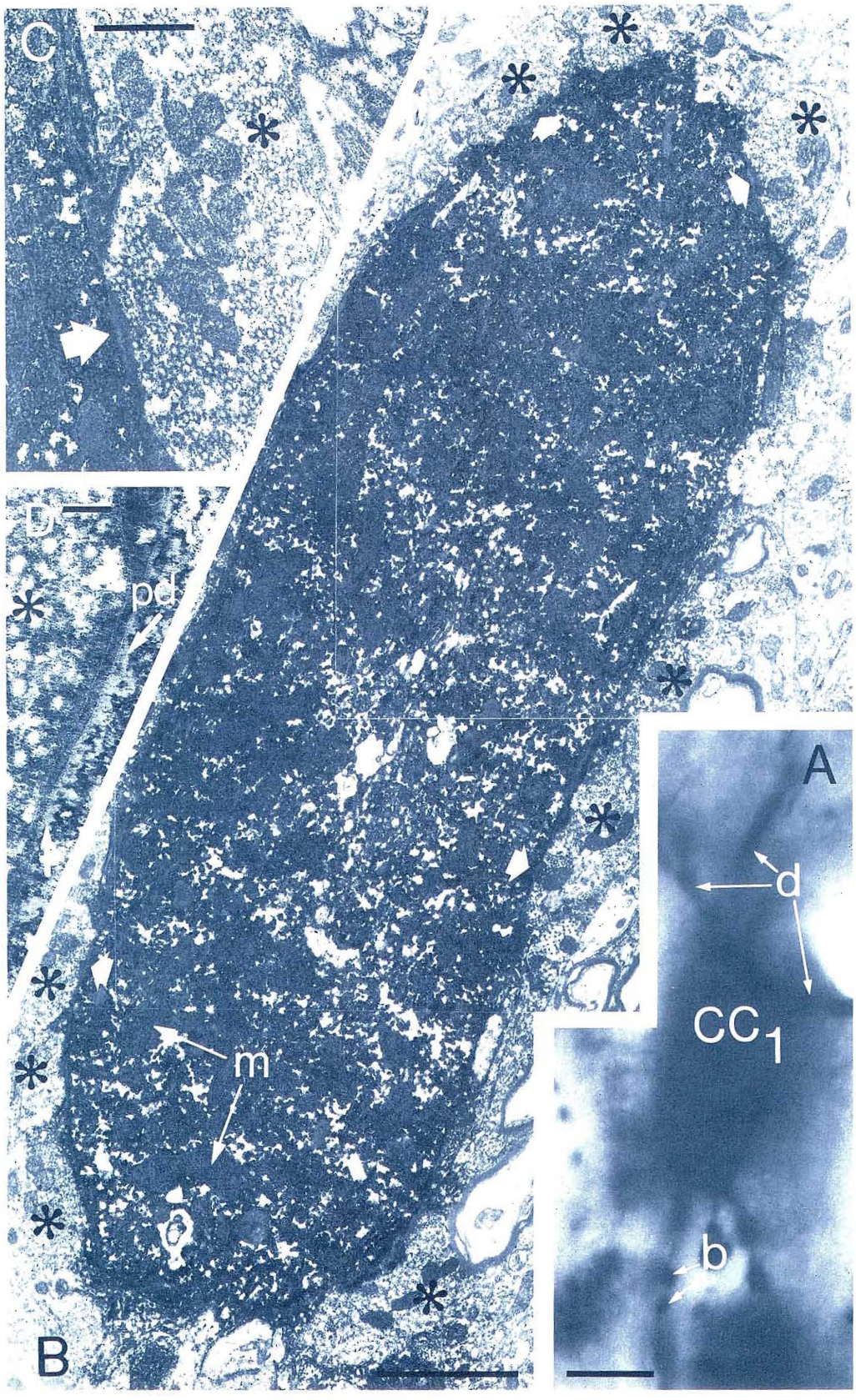

Fig. 7. Clutch cell No. 1. A. Light micrograph of the perikaryon (CC_1) with emerging dendrites (d), and boutons (b) of an axon collateral. B. Electron micrograph of the same somata, surrounded by large boutons (asterisk). They made synaptic contacts (large arrows) in this or in subsequent sections. The cell is rich in mitochondria (m). C. One bouton making an axosomatic synapse (arrow) with the cell is shown at higher magnification. The bouton (asterisk) contains uniform round vesicles. D. The postsynaptic density (pd, arrows) at the synaptic junction of another bouton (asterisk) is "negatively stained" and indicates a type I contact. Scales: A, 10 μm; B, 2 μm; C, 0.5 μm; D, 0.1 μm.

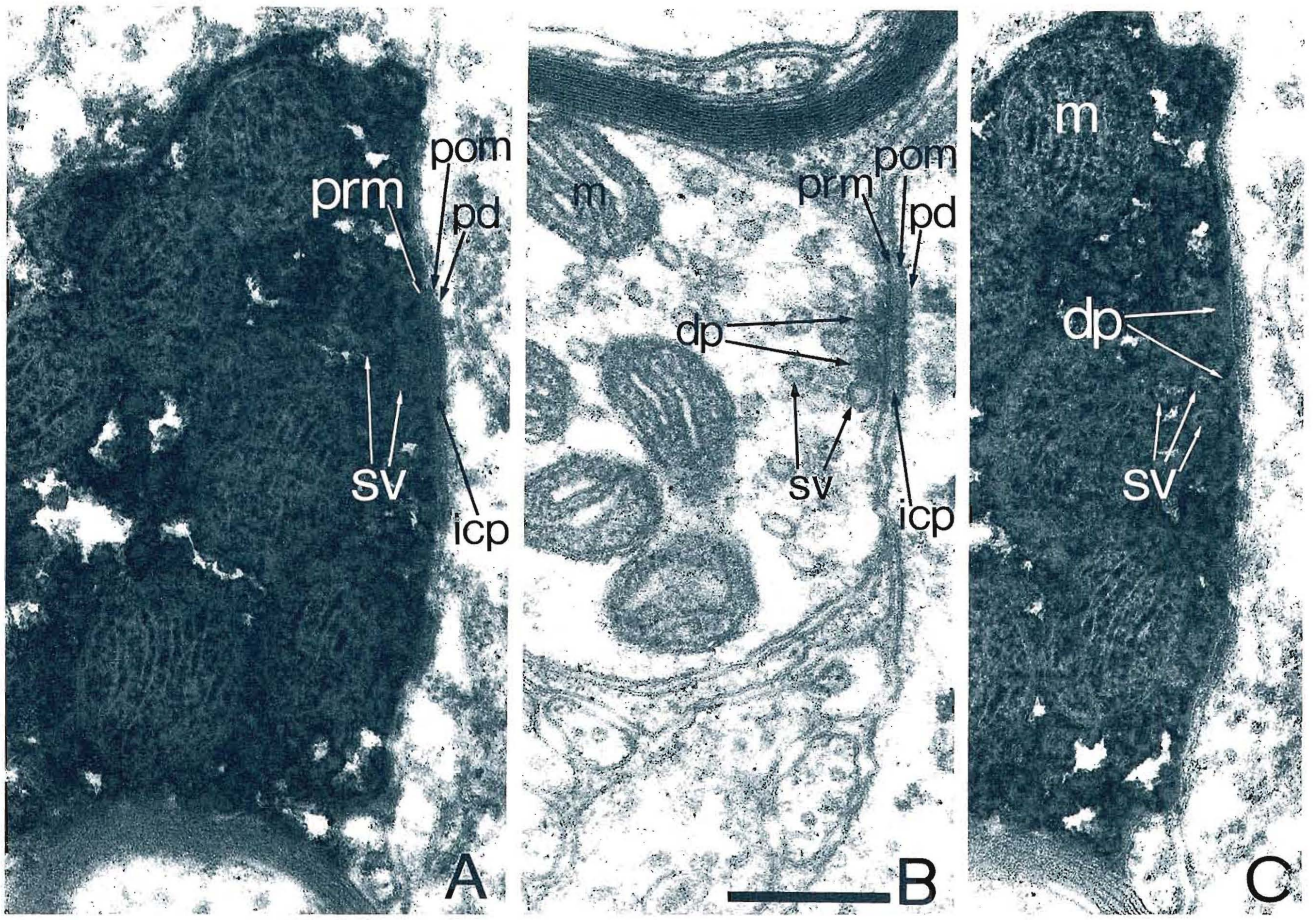

Fig. 8. Comparison of fine structural features of a type II synaptic junction (B) with the features recognisable at the junction formed by an HRP-filled bouton of clutch cell No. 1 (A and C, serial sections). Both boutons formed synapses with the same type P soma in layer IVa. At the junction the extracellular space is widened and the pre (prm)- and postsynaptic (pom) membranes are rigidly apposed. The intercellular plaque (icp), membranes of synaptic vesicles (sv), mitochondria (m), presynaptic membrane (prm), and presynaptic dense projections (dp) appear negatively stained as they are not penetrated by the reaction endproduct. There is only a very small postsynaptic density (pd) at these synapses in layer IV. Scale: A–C, same magnification, 0.2 μm.

lacelike appearance (Figs. 9A, 10A, 13A). The boutons contained large groups of mitochondria and pleomorphic vesicles. The latter could be recognised because their membranes were negatively stained by the HRP reaction endproduct (Figs. 8, 9G,H, 10C,D, 11B,D, 13B,E). The recognition of vesicle clustering (Fig. 10D) and the negative staining of presynaptic dense projections (Fig. 8) helped to identify synaptic contacts (Figs. 9G, 10C, 11B, 12C–F). The boutons formed very small type II synaptic junctions with small postsynaptic densities (e.g., Figs. 8, 9G,H, 11D, 12). The HRP reaction endproduct sometimes spread into the extracellular space around boutons, often also filling the synaptic cleft (e.g., 9H, 12,A,B,F) but leaving the intercellular plaque recognisable (Fig. 8). In addition to the HRP-filled boutons, other boutons of very similar character were contacting the same postsynaptic neurons. A comparison of the fine structural features of HRP-filled and -unfilled boutons is shown in Figure 8. All the features were not always present in every section of synapses formed by HRP-filled boutons. The reaction endproduct made it more difficult to identify synaptic contacts from single sections. However, all contacts were identified from several serial sections and the small postsynaptic density (e.g., Figs. 8, 12A,B,C), the slightly widened extracellular space (Figs. 8, 9H, 10D) at the junction, or the other features shown in Figure 8 served to identify the synaptic contacts.

Postsynaptic elements. Two of the cells, CC1 and CC2, were analysed extensively, but only four boutons were studied from the axon of CC3. A total of 321 boutons were serially sectioned in area 17. Of these, 273 boutons were drawn from a random sample. The distribution of their postsynaptic targets is shown in Figure 20. An additional 48 boutons that contacted somata were sectioned, for subsequent testing of the GABA immunoreactivity of the postsynaptic somata. These data are not included in Figure 20.

We were interested in estimating the total number of elements in synaptic contact with the axon of CC1 in layer IV. In the light microscope, 1,083 boutons were seen to contact 434 somata; the remaining 1,650 boutons were in the neuropil. A sample of 45 of the boutons contacting the

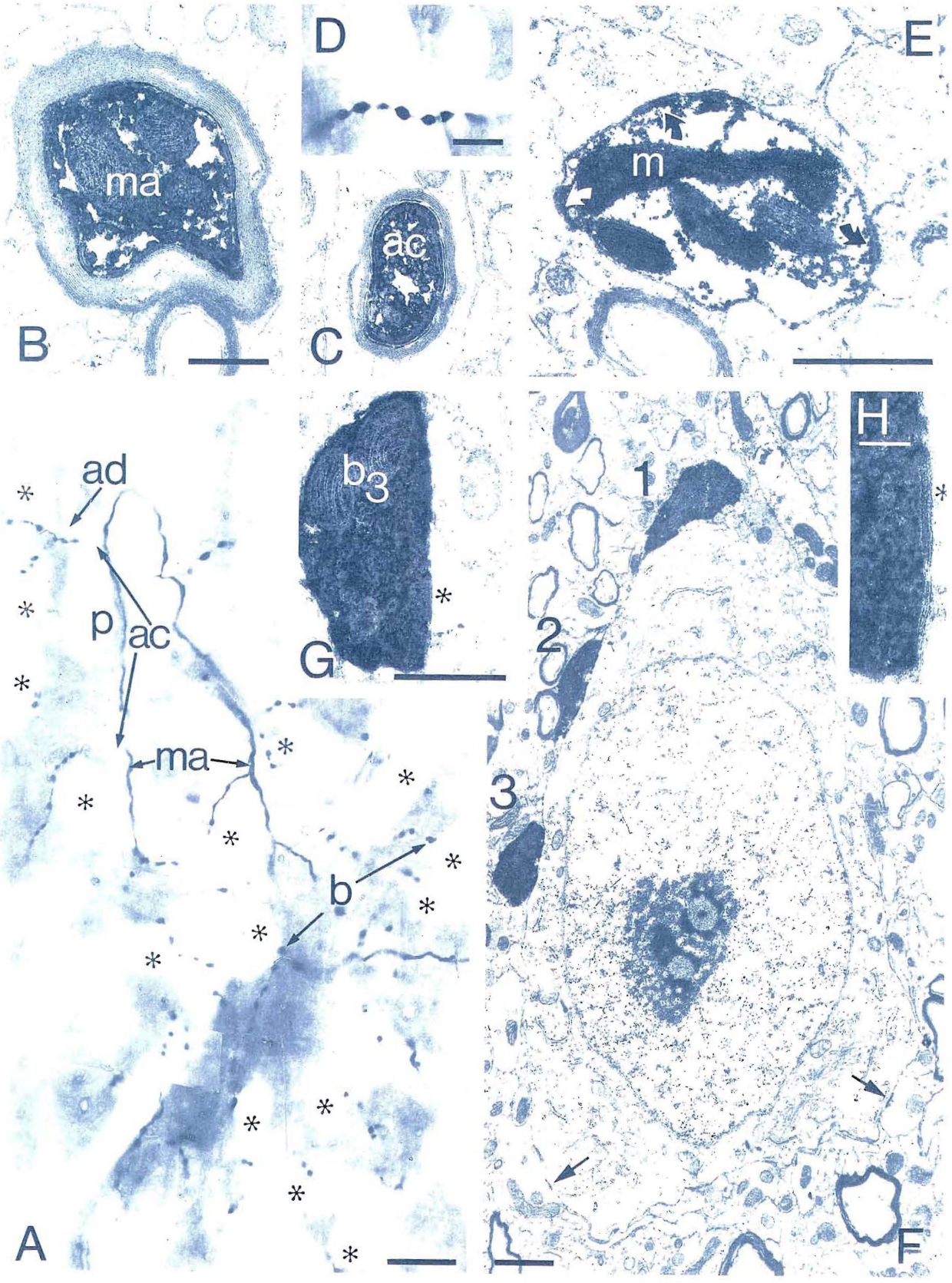

Figure 9

somata were examined in the electron microscope and some of these made additional synapses on spines and dendrites, giving an average of 1.2 postsynaptic elements per bouton. A sample of 102 boutons from the neuropil fraction showed that these boutons made synapses with an average of 1.28 elements. Extrapolating from these samples, we estimated that CC1 made synaptic contacts with 3412 elements, and that 31.7% of the synapses were axosomatic. The calculation was applied only to layer IV because the density of neuronal somata in layer V and VI was different from that in layer IV and CC1 had a relatively small (143 boutons) projection to the deep layers.

Direct electron microscopic analysis was carried out to identify the postsynaptic structures (Fig. 20). The four boutons examined in area 18 made synaptic contacts with two dendrites and two type P (see below) somata. We have not pursued the synaptic connections of CC3 further because the preservation of the tissue was not optimal and because very little is known about the cellular elements of layer IV in area 18. In the following the fine structural features of the synaptic targets in area 17 will be described for CC1 and CC2 together.

Somata. They constituted 24.5% of the postsynaptic structures made by CC1 in layer IV (Fig. 20). This is lower than that obtained from the light microscopic estimate (31.7%) but nevertheless, considering the sample size (6.6% of all boutons were serially sectioned for the random sample), the two estimates are close. In layer V, only 6% of the boutons made synapses with somata on the basis of electron microscopic counts. Of the 99 synapses of CC2 only 19% were made on somata in layer IV. Individual somata could be contacted by one to five boutons.

The postsynaptic somata were heterogeneous in their shape, size, and fine structural appearance (Figs. 9–11, 14). In spite of studying long section series, only two broad categories, P-type neurons and S-type neurones, could be established. Within the P category (pyramidallike) differences are apparent e.g., (compare Figs. 10B and 11A) but it has been impossible to find distinctive qualitative features which would allow categorical separation. Type P somata were radially elongated and often pyramidal shaped (Figs. 9F, 11A) or oval (Fig. 10B). Each had a large nucleus, prominent nucleolus, light cytoplasm, and sparse cytoplasmic organelles. The dendrites originated by conical tapering from the soma. Frequently a major apical dendrite of variable thickness could be seen directed toward the pia (Figs. 11A). Type P cells received exclusively type II synaptic boutons on their soma. The number of axosomatic synapses observed in one section was low, usually zero to three rarely up to five (Figs. 9F, 10B). The unidentified boutons and the HRP-filled clutch cell boutons made similar synaptic contacts and were similar in size and shape, suggesting convergence of a number of clutch cells on the same target. The same neurons that received clutch cell boutons on their soma could also receive synaptic contacts on their proximal dendrites (Fig. 10B).

From electron microscopic examination alone we can not be sure of the identity of the individual neurons. However, their shape, the orientation of their dendrites, and their somatic synaptic input strongly suggest that they include the spiny neurons of layer IV. The identification is made difficult because three types of neuron could be expected to give the electron microscopic profiles: (1) pyramidal cells with apical dendrites ascending to layer I, (2) star pyramidal cells with rudimentary apical dendrites often ending in layer III, and (3) spiny stellate cells with dendrites remaining in layer IV but nevertheless having a major dendrite directed toward the pia. All these cells have been observed in intracellular electrophysiological and Golgi studies of layer IV (Szentágothai, '73; Lund et al., '79; Gilbert and Wiesel, '79, '83; Peters and Regidor, '81; Lund, '84; Martin and Whitteridge, '84). Their somatic input is probably similar (LeVay, '73; Mates and Lund, '83). More detailed work is needed in the cat on identified spiny neurons before particular cell types can be correctly identified only from electron microscopic examination alone, but it is noteworthy that our type P somata were not similar to any of the four types of [^{3}H]-GABA-accumulating neurones studied in layer IV of the cat's striate cortex (Hamos et al., '83). On the basis of the present observations and data from the literature (LeVay, '73; Davis and Sterling, '79; Hornung and Garey, '81), it is likely that the type P category includes spiny stellate cells (Fig. 10) and star pyramidal and pyramidal cells (Figs. 9F, 11A).

These spiny cells are thought to be excitatory. Thus it was some support for our categorisation that none of the type P cells that were postsynaptic to clutch cells showed GABA immunoreactivity (Table 4). Although negative results in immunocytochemistry have to be treated with caution, there are good technical reasons for concluding that the P-type neurons are not GABAergic: (1) the GABA procedure requires no colchicine treatment for staining of somata, (2) the postembedding method has no penetration problems, (3) there is good agreement between GAD and GABA immunostaining (Somogyi et al., '84). All postsynaptic type P cells in the present study were contacted by GABA-immunoreactive varicosities (Fig. 17C) which have been shown to be synaptic boutons with type II junctions (Somogyi and Hodgson, '85).

A few postsynaptic somata (Table 4; one for CC1 and one for CC2 in the random sample) were conspicuously different and were thought to represent smooth dendritic neurons. These neurons were placed into the type S group (Fig. 20). One (Fig. 11C,D) had a high cytoplasm-to-nucleus ratio, was densely packed with mitochondria, and had many secondary lysosomes. This neuron was densely covered by both type I and type II synapses, and may correspond to the type 1 [^{3}H]-GABA-accumulating neurones of Hamos et al. ('83). Another two cells were also very densely covered by synaptic boutons and contained a conspicuously large amount

Fig. 9. Clutch cell No. 1. A. Photomontage of a part of the axon in layer IV. A. The main myelinated axon (ma) emits thin axon collaterals (ac) which are studded with large boutons (b). Some of the boutons are in the neuropil but others surround neurons (asterisks) of various sizes and shapes. Only one of them (p) has a typical apical dendrite (ad). B,C. Electron micrographs of the main axon (ma) and an axon collateral (ac) shown at the same magnification. Note the difference in the thickness of the myelin sheath. D. Light micrograph of a beaded dendrite. E. Electron micrograph of a swelling on a distal dendrite containing mitochondria (m) and receiving synaptic contacts (arrows) from small boutons. F. Electron micrograph of a pyramidal-shaped somata contacted by three labelled boutons (1–3) and receiving synapses (arrows) from two unlabelled boutons in layer IVA. G. One of the boutons (b_3), shown in F, is seen to make type II synaptic contact (asterisk) in a serial section. H. The synaptic junction of b_3 (asterisk) can be recognised from the widened cleft and other features described in Figure 8. Scales: A, 20 μm; B,C,E,G, 0.5 μm; D, 10 μm; F, 1 μm; H,0.1 μm.

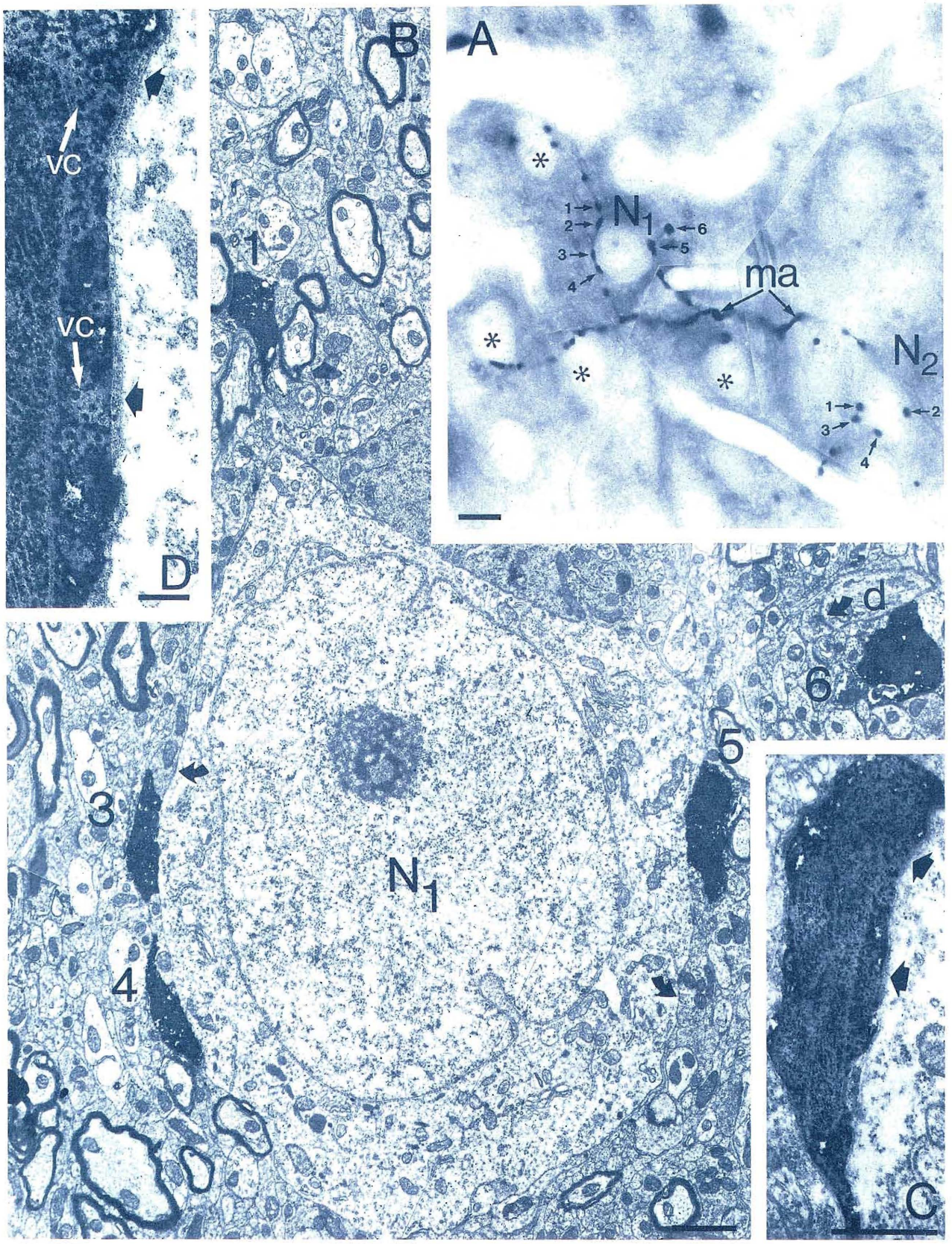

Fig. 10. A. Light micrograph of the axon clutch cell No. 1. The myelinated axon collateral (ma) emits varicose terminal segments which surround small somata (asterisks) in layer IV. B. Two of the somata (N_1 and N_2) are associated with six and four boutons, respectively, and are shown on electron micrographs in B and Figure 9A. A light micrograph of N_1 has been published by Martin et al. ('83). B. Electron micrograph of the same neuron (N_1) as shown in A. Complete serial sectioning of the neuron showed that boutons Nos. 2–5 made synapses with the soma, while boutons Nos. 1 and 6 made synapses with proximal dendrites (d). Both the soma and the dendrites received additional synapses (curved arrows) from unidentified boutons. C. Serial section to that shown in B of bouton No. 2 in synaptic contact (arrows) with the soma. D. Higher-magnification view of the synaptic junctions (arrows) shown in C. The junctions can be recognised on the basis of the widened extracellular cleft and the vesicle clusters (vc). Scales: A, 10 μm; B, 1 μm; C, 0.5 μm; D, 0.1 μm.

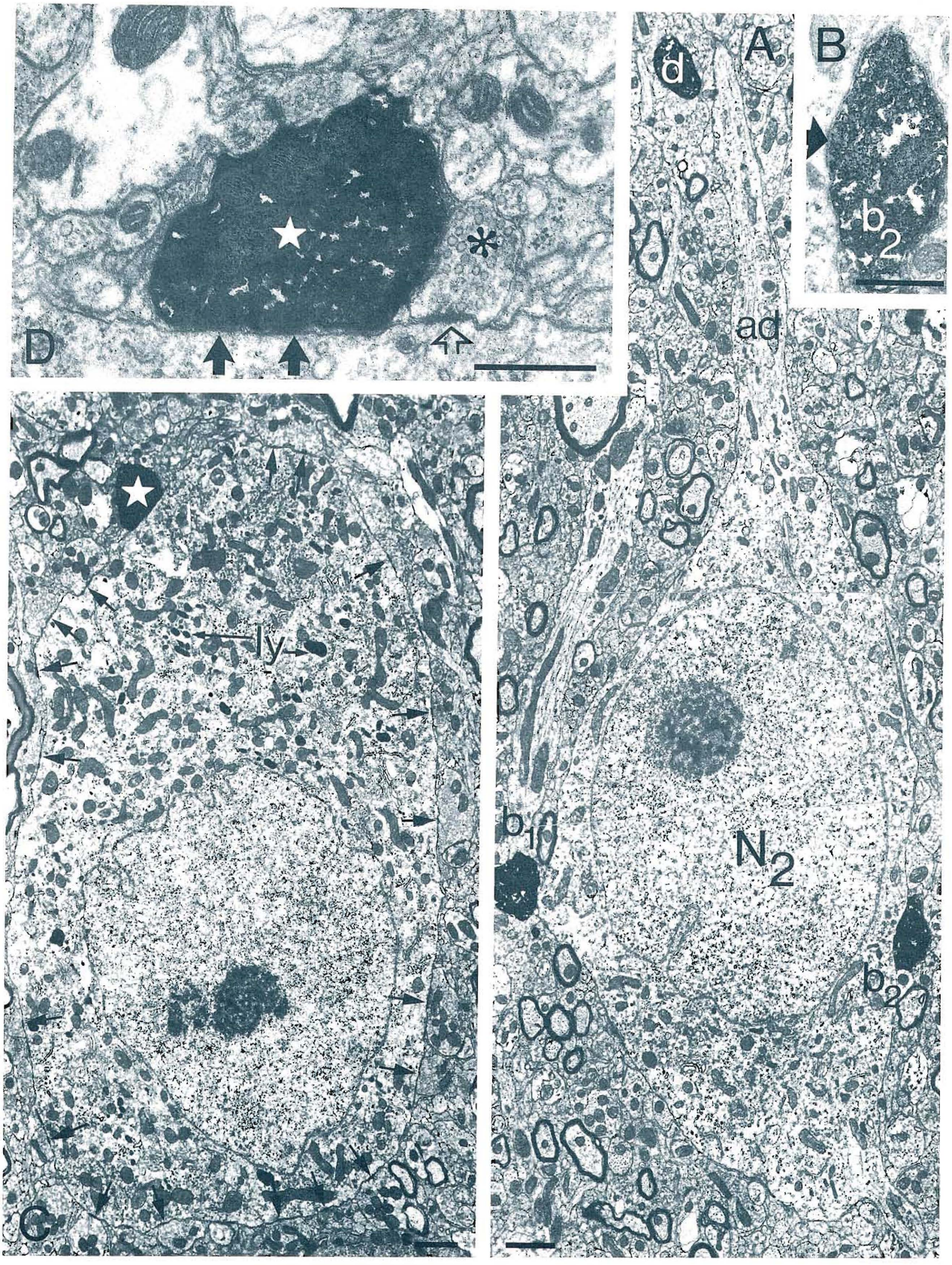

Fig. 11. Different types of neurons postsynaptic to clutch cell No. 1. A. Pyramidal-shaped neuron (N_2) contacted by two HRP-filled boutons ($b_{1,2}$) and also shown in light micrograph in Figure 7.A. The neuron has an apical dendrite (ad) passing near one of the HRP-filled dendrites (d). B. One of the boutons (b_2) is shown at higher magnification in synaptic contact (arrow) with the somata from a consecutive section. C. A nonpyramidal neuron receiving a very large number of synaptic contacts (arrows) on its somata. One of them (star) originates from the clutch cell. The soma contains a high density of mitochondria and secondary lysosomes (ly). D. Serial section of the same labelled bouton (star) as in C making a type II synaptic contact (arrows) with the soma. An unidentified bouton (asterisk) containing round vesicles also makes a synaptic junction (open arrow). Scales: A and C, 1 μm; B and D, 0.5 μm.

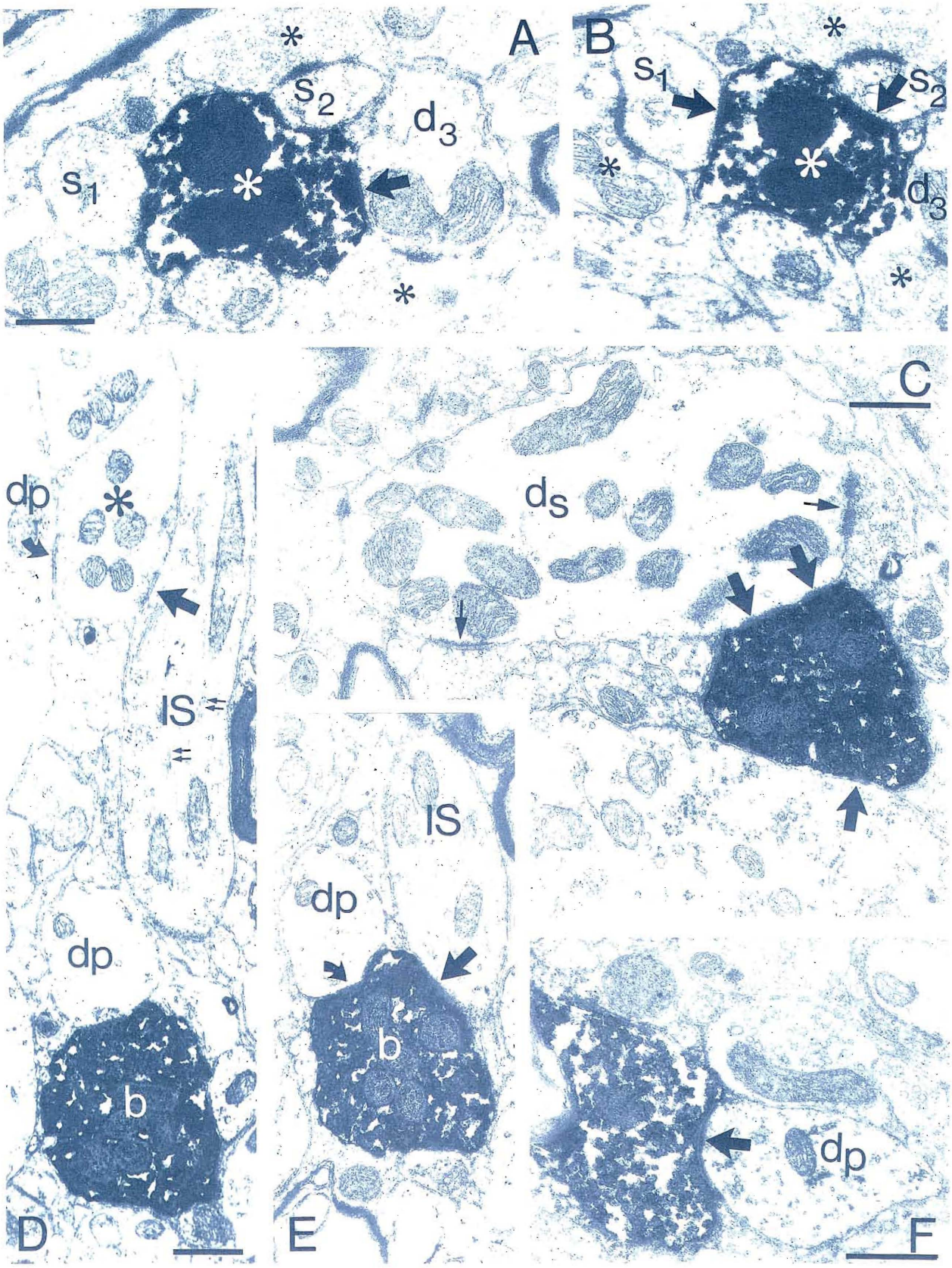

Fig. 12. Different types of elements postynaptic to HRP-filled boutons of clutch cell No. 1. A,B. Serial sections of two spines (S_1,S_2) and a dendrite (d_3) receiving type II synapses (arrows) from the same identified bouton (white asterisk) as well as type I synapses from unidentified boutons (black asterisks). C. Type S dendrite (d_s) receiving two synapses (small arrows) from unidentified boutons and one synapse (large arrows) from the HRP-filled bouton which also contacts a soma (arrows). D,E. Serial sections illustrating an axon initial segment (IS) receiving synaptic contacts (large arrows) from an unidentified (asterisk) and an HRP-filled bouton (b). Both boutons make synaptic contacts (curved arrow) with nearby type p dendrites as well. The initial segment was traced back to a pyramidal cell and contains the characteristic microtubule fascicles (small arrows). F. A small type p (d_p) dendrite, receives synaptic contact (arrow) from an HRP-labelled bouton. Scales: 0.5 μm; A,B same magnification; D–E, same magnification.

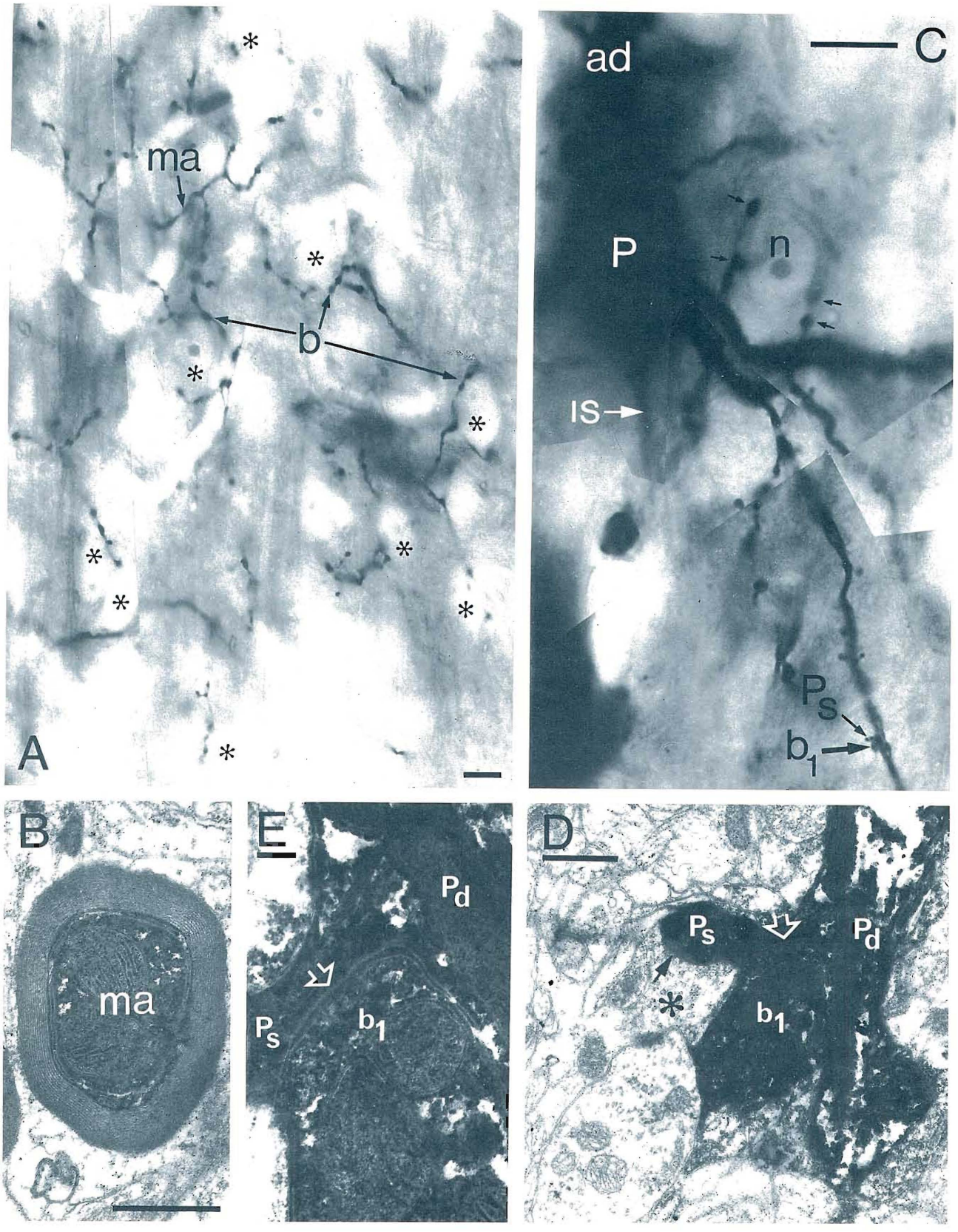

Fig. 13. A. Light micrograph of the axon arborisation of clutch cell No. 2 in layer IV. The main myelinated axon (ma) emits collaterals crowded with large boutons (b) some of which contact perikarya of neurons (asterisks) having various sizes and shapes. B. Electron micrograph of one of the main axons (ma) surrounded by a thick myelin sheath. C. Photomontage of the large pyramidal cell (P) which was filled with HRP together with the axon of clutch cell No. 2. The axon initial segment (IS) the apical dendrite (ad) and basal dendrites are shown. Boutons (small arrows) of the clutch cell contact a neuronal somata (n) and also one bouton (b_1) that was apposed to the basal dendrite next to a spine (Ps). D,E. Electron micrographs of the clutch cell bouton (b_1) shown also in C, as it makes a synaptic contact (open arrow) with the pyramidal cell basal dendrite (Pd) and the neck of the spine (Ps). The spine also receives a type I contact (arrow) from another bouton (asterisk). Scales: A and C, 10 μm; B and D, 0.5 μm; E, 0.1 μm.

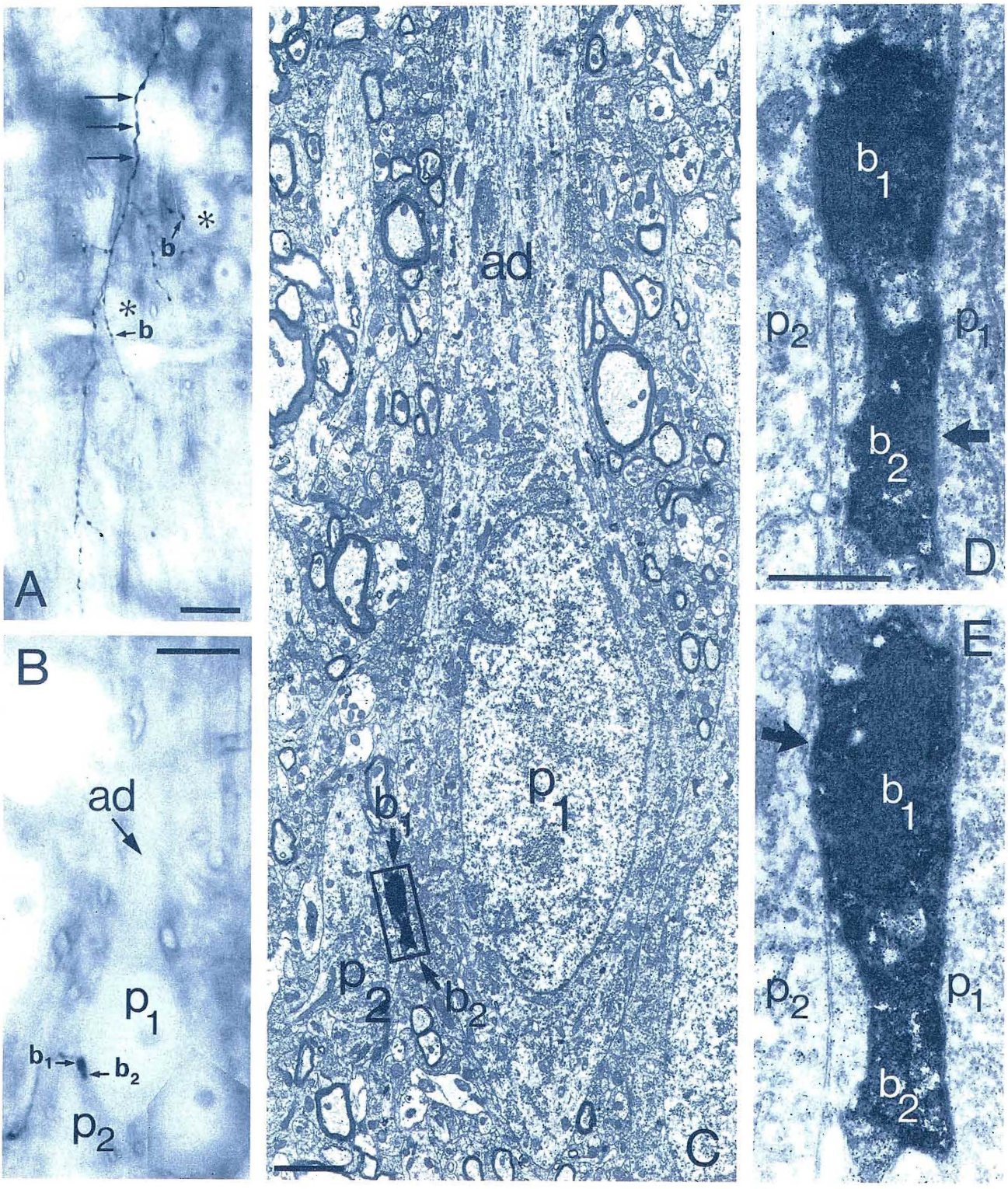

Fig. 14. A light micrograph photomontage of a collateral of clutch cell No. 2 descending to layer V. The main collateral (arrows) was myelinated. Some boutons (b) of the varicose secondary collaterals approach neuronal somata (asterisk). B. Light micrograph of two boutons (b_1b_2) in apparent contact with a pyramidal cell (p_1) in layer V. The prominent apical dendrite (ad) and another pyramidal cell (p_2) below the plane of focus are indicated. C. Electron micrograph of the same area shown in B. The two HRP-labelled boutons (b_1, b_2) are seen in apposition to the soma of p_1 and to the tip of p_2. Framed area is shown in serial sections in D and E at higher magnification. D,E. The two boutons (b_1, b_2) of clutch cell No. 2 make synaptic contacts (arrows) with both pyramidal neurons (p_1, p_2). Scales: A, 20 μm; B, 10 μm; C, 2 μm; D and E, 0.5 μm.

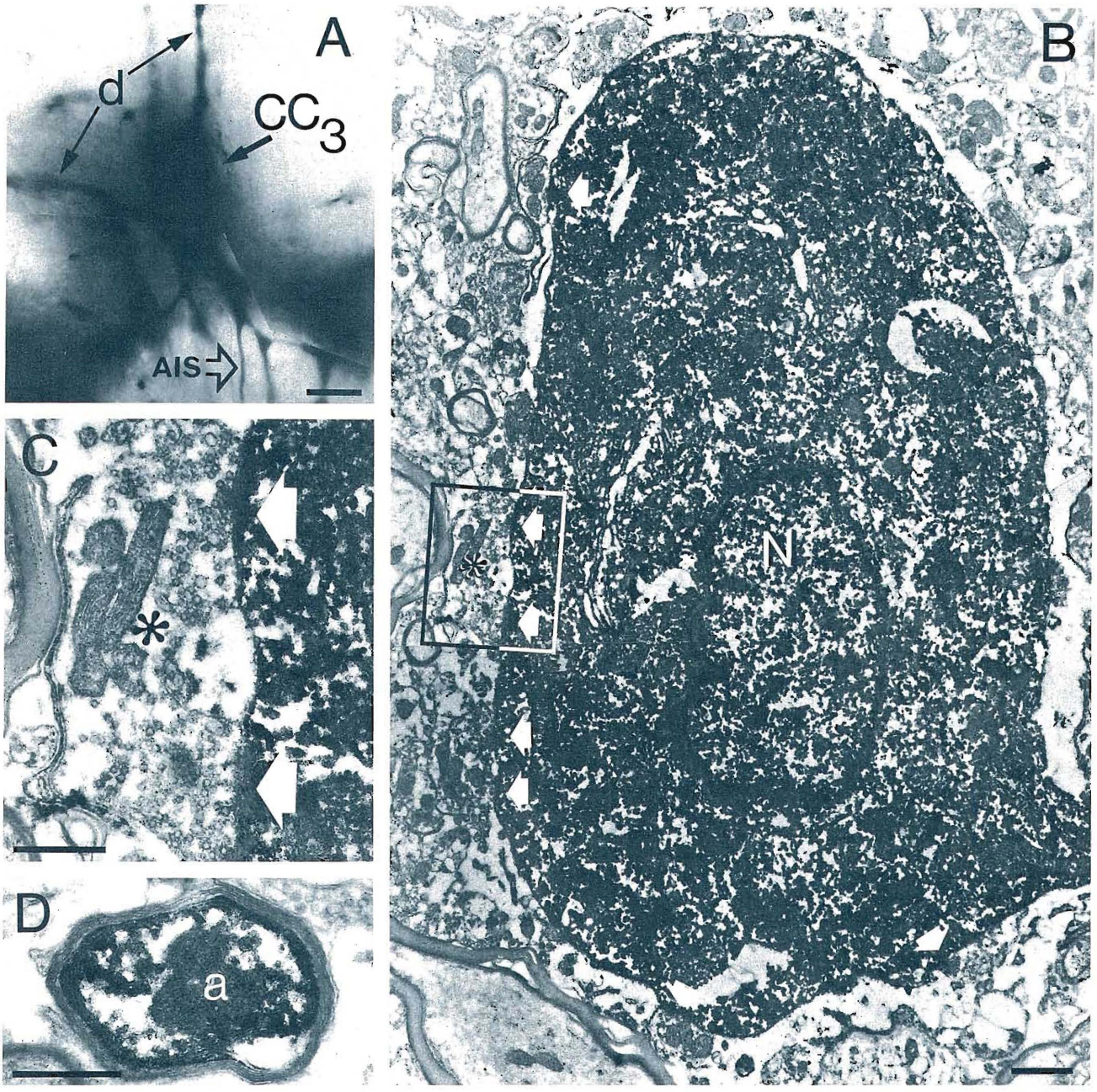

Fig. 15. Clutch cell No. 3 in area 18. A. Light micrograph of the perikaryon (CC_3) with emerging dendrites (d) and axon initial segment (AIS) originating from one of the main dendritic shafts. B. Electron micrograph of the soma with an eccentrically placed nucleus (N). Some oedematous tissue damage around the plasmalemma is apparent, but boutons making axosomatic synapses (white arrows) can be identified. One large bouton (asterisk) in framed area is shown in C at higher magnification. C. The large bouton (asterisk) containing spherical vesicles makes multiple synaptic contacts (arrow) with the soma. D. A main axon collateral (a) is seen enveloped by a thin myelin sheath. Scales: A, 10 μm; B, 1 μm; C and D, 0.5 μm.

of rough endoplasmic recticulum extending into the dendrites. The axon initial segment of a fourth neuron was directed toward the pia and also had a high cytoplasm-to-nucleus ratio (Fig. 17A). All the above features have been observed on identified aspinous, nonpyramidal cells (see Peters and Saint Marie, '84) many of which are thought to be GABAergic. For the neurones contacted by clutch cells this was directly confirmed in the present study by post-embedding GABA immunohistochemistry (Fig. 17, Table 4). Because the anti-GABA serum was developed at a late stage of this study we could not test neurones which had already been completely cut for electron microscopy in the random sample. The small proportion of GABA-positive cells amongst the targets of clutch cells shows that GA-

BAergic neurons, which probably correspond to S-type cells, are a minor target of clutch cells in layers IV and V (Table 4).

Dendrites. Dendrites were the most frequent target in layer IV, making up 44.3% of the postsynaptic elements for CC1 and 52.2% for CC2. In layer V for CC1 they constituted 60% of the targets. Some dendrites could be traced back to their parent cells (Fig. 10B,C) and thus identified as originating from P- or S-type neurons. Most of the dendrites, however, were just isolated profiles, which made it difficult to determine their origin. Similarly to the postsynaptic perikarya, two broad categories of postsynaptic dendrites were recognised.

Type P dendrites had light cytoplasm, contained few mitochondria, and received few synapses from boutons other than the HRP-filled one (Figs. 12A,B,D–F, 19). They were similar to the dendrites originating from type P somata. Some type P postsynaptic dendrites were radially oriented, like that originating from the type P cell in Figure 11A and they were assumed to be apical dendrites of pyramidal cells. On one occasion the synaptic contact was on a sidebranch of such a dendrite. Type P dendrites constituted the majority of the postsynaptic dendritic shafts. Qualitatively, type P dendrites were very similar to the type P dendrites that received synapses from large basket cells in layer III of area 17 (Somogyi et al., '83). However, quantitative comparison of their size showed that those receiving clutch cell input in layer IV were significantly smaller (Fig. 18).

Further evidence that type P dendrites belong to the spiny neurons was obtained from the HRP-injected pyramidal neuron that sent its basal dendrites within the termination area of CC2. Four boutons of CC2 contacted the dendrites, and in one case we proved by electron microscopy that the clutch cell bouton directly contacted the dendrite and the neck of a spine (Fig. 13C–E). Both the dendritic shaft and the spine neck received synaptic contact, although the dense reaction end product also filled the synaptic cleft.

Type S postsynaptic dendrites contained numerous mitochondria and received a large number of synapses, mainly type I (Fig. 12C). They were similar to the dendrites emerging from type S neuronal somata and to dendrites described previously as belonging to smooth and sparsely spiny neurons (Davis and Sterling, '79; Hornung and Garey, '81; Somogyi et al., 83a,b). They made up 8% (CC1) and 9% (CC2) of the postsynaptic elements in layer IV (Fig. 20).

Quantitative comparison of type P and type S dendrites was made on the basis of the synaptic coverage and mitochondrial density (Fig. 19). Type P dendrites formed a tight cluster indicating that they were more homogeneous than type S dendrites, which showed greater scatter. The dendrites of CC1 were similar to type S dendrites, indicating again that type S dendrites probably belong to neurons with smooth dendrites. Five percent of the dendrites postsynaptic to CC1 in layer IV, 6% in layer V, and 8% postsynaptic to CC2 could not be classified as P or S type (Fig. 20). They were not included in Figure 19.

Spines. Spines were identified on the basis of spine apparatus, the lack of mitochondria, or from serial sections showing them as having a head and a stalk (Fig. 12A,B). Spines were an important target for both CC1 (30.6%) and CC2 (26.3%) in layer IV, and also for CC1 in layer V (34%). It was not possible to establish the origin of the spines because very few could be traced back to type P dendrites. Interestingly, every spine received a type I synaptic contact

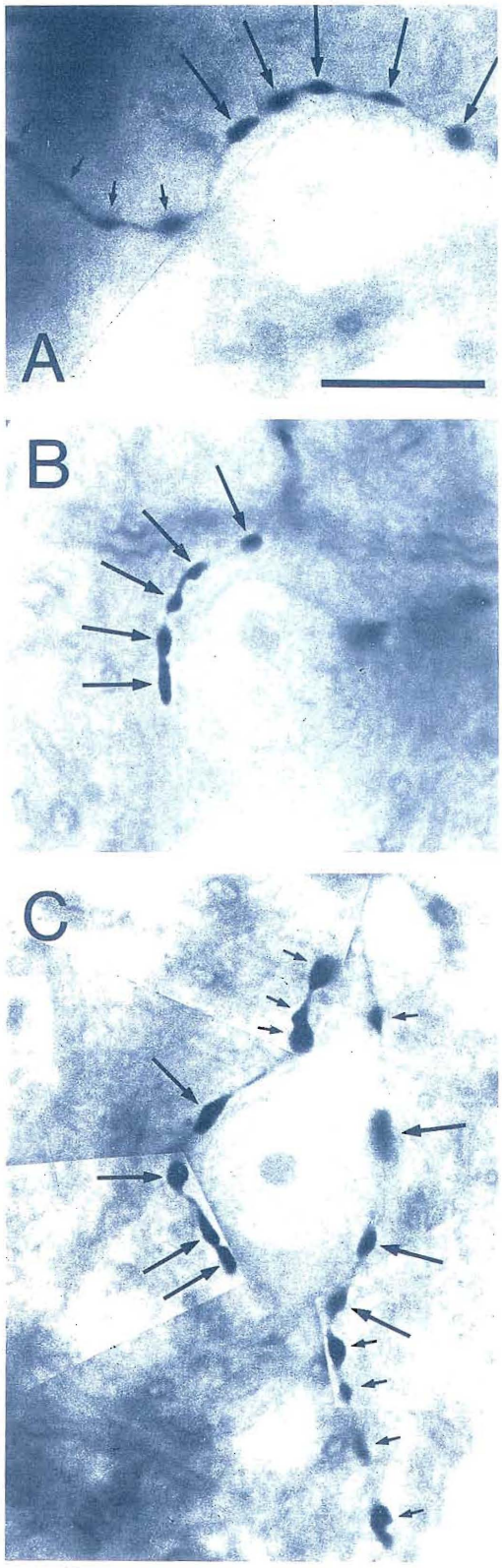

Fig. 16. Light micrographs of neurons in contact with boutons of clutch cell No. 3 in layer IV of area 18. Only some boutons (long arrows) are near the somata; others (short arrows) are in the neuropil. Scales: A–C, same magnification, 10 μm.

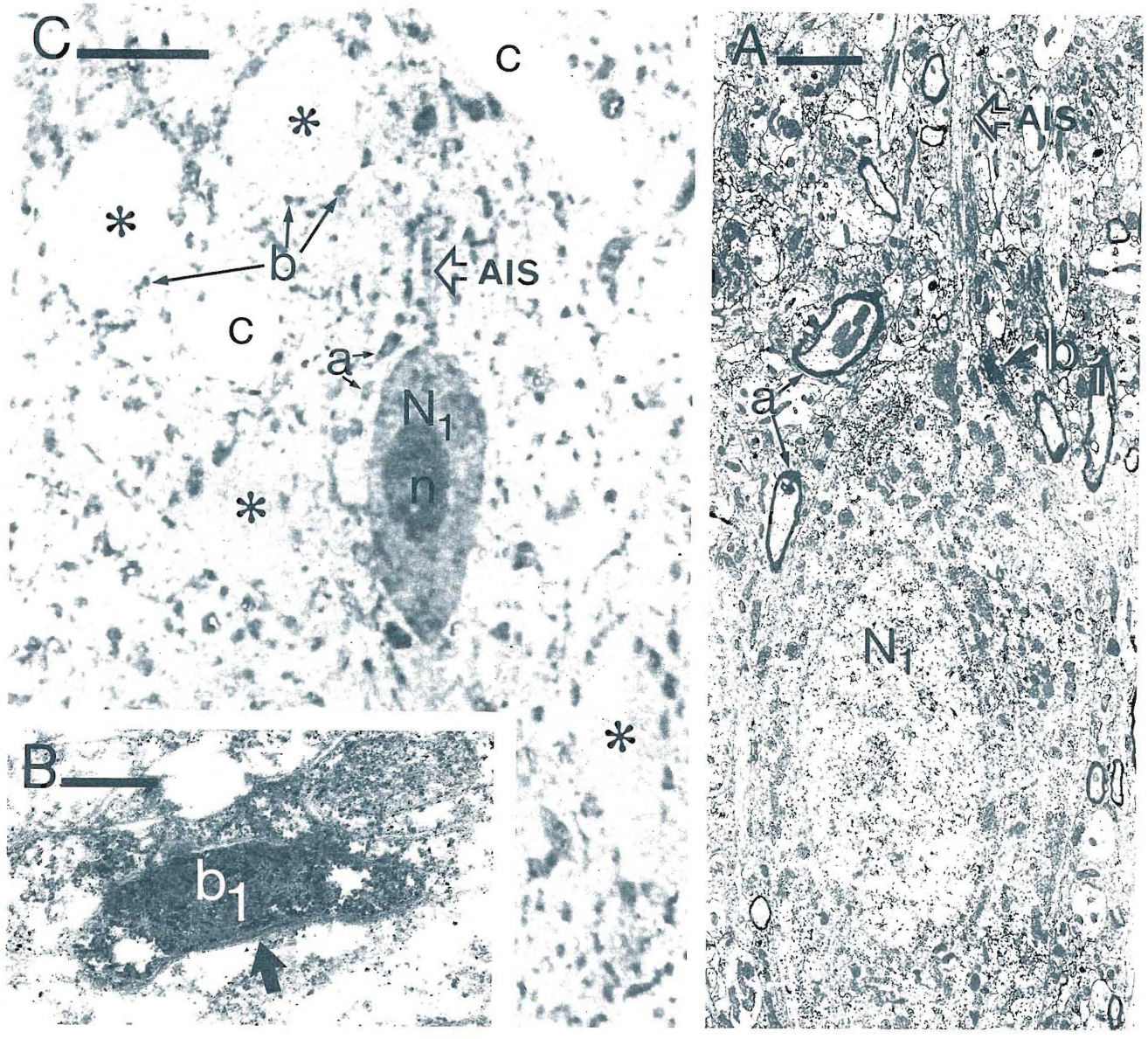

Fig. 17. Immunocytochemical demonstration of GABA in a neuron postsynaptic to clutch cell No. 2, and situated at the top of layer IVA. A. Electron micrograph of the postsynaptic somata (N_1) contacted by the HRP-labelled bouton (b_1). Note the axon initial segment (AIS) is directed toward the pia. B. The HRP-filled bouton (b_1) is shown at higher magnification, in synaptic contact (arrow) with the somata. C. Light micrograph of a 0.5-μm-thick section treated to reveal GABA. The neuron (N_1) shown in A is immunoreactive, including its nucleus (n), while neighbouring neurons (asterisk) are negative for GABA. Immunoreactive boutons (b), some surrounding neuronal somata (arrows) and immunoreactive axons (e.g., a), are also demonstrated. c, capillaries. Scales: A, 2 μm; B, 0.2 μm; C, 10 μm.

from boutons containing round synaptic vesicles in addition to the type II contact established by clutch cells (Fig. 12A,B, 13D,E).

Axon initial segments. Four postsynaptic profiles could be identified as axon initial segments (Figs. 12D,E, 20) on the basis of microtubule fascicles and electron-dense membrane undercoating (Palay et al., '68). Only one of them received another type II synaptic contact from a similar bouton which also contacted dendrites (Fig. 12D). These axon initial segments were not as densely covered with synapses as they are in layer III (Fairén and Valverde, '80; Freund et al., '83).

Postsynaptic targets in layer V. Although the vast majority of boutons were in layer IV, all clutch cells gave descending collaterals to layer V. This gave an opportunity to study whether clutch cells really give synapses to pyramidal cells since these can be recognised unequivocally in layer V because of their massive apical dendrites. Some (6% for CC1) of the boutons of both clutch cells established synapses with somata of pyramidal cells (Figs. 14, 20).

TABLE 4. Neurochemical Characterisation of Postsynaptic Perikarya to Neurons CC1, CC2, and CC3[1]

No. of neurons	Cortical layer	No. of GABA-positive somata[2]	No. of GABA-negative somata[3]	Total
CC1	IV	1 (1)	36 (19)	40
	V	0	3	
CC2	IV	3 (1)	21 (7)	24
CC3	IV	0	2	2

[1]Neurons were tested by postembedding GABA immunocytochemistry, including random (in parentheses; synaptic data in Table 2) and non-random samples.
[2]All GABA-positive cells were of the S type.
[3]All GABA-negative cells were P type on the basis of fine structural criteria.

Spines (34%) and type P dendrites (50%) were the majority of the postsynaptic targets in layer V. Since here they very likely belong to pyramidal neurons, it is evident that besides the layer IV neurons, a localised group of layer V pyramidal cells also receive input from layer IV clutch cells.

DISCUSSION

Definition of clutch cells

Clutch cells can be identified on the basis of the following characteristics: somata in layer IV; smooth dendrites; very dense rectangular axonal arborisation (300 × 500 μm), largely restricted to layer IV; large bulbous boutons; short interbouton intervals; they establish type II efferent synaptic contacts; 20–30% of their synapses are given onto layer IV somata, most of which are not immunoreactive for GABA; they also form synapses with dendritic shafts (35–50%) and spines (30%).

Clutch cells in previous studies

Undoubtedly our sample is small, but these cells are rarely encountered in either intracellular filling or in Golgi studies. The three neurons for the present study are a result of 4 years of intracellular filling of hundreds of neurons in the cat. In the cat, only one example of a clutch cell has been found in the Golgi literature (Lund et al., '79 of Fig. 6B). This is not surprising in light of the present results showing that most of the main axons of clutch cells are myelinated in the adult cat, rendering them largely inaccessible for Golgi impregnation. In the kitten, where myelination is probably less extensive, Lund et al. ('79) described these neurons throughout layer IV. Similar neurons have been described in layer IV of the primate visual cortex (Ramón Cajal, 1899; Valverde, '71,'78; Lund, '73; Mates and Lund, '83) and they seem to be associated in particular with layer IVC. In this layer, it has been shown that they form type II synaptic contacts with somata (Mates and Lund, '83).

Similarly, in the kitten Lund et al. ('79) called attention to the association of the terminals of these cells with the somata of other neurons. This has been confirmed in the present study and it has also been shown that the boutons form type II synaptic contacts.

The target neurons of clutch cells

The electron microscopic data strongly suggest that the major targets are the different parts of spiny cells in layer IV. Pyramidal cells of layers V and III and GABAergic neurons formed only a minority of the postsynaptic elements. Because the somatic features and synaptic input of identified spiny neurons have not been studied in detail in the cat, it is not yet possible to establish if any of the three major classes—the spiny stellate, star pyramidal, and pyramidal cells—can be excluded as targets. The significant differences in the thickness of postsynaptic type P dendrites, contacted by clutch cells in layer IV and large basket cells in layer III, respectively, indicates that different neuronal populations receive the input from the two cell types. The thinner dendrites in layer IV could belong to spiny stellate and star pyramidal neurons, which are smaller than layer III pyramidal cells.

The overall distribution of clutch cell synapses on different targets is very similar to that of the large basket cells (Somogyi et al., '83b). While large basket cells contact only a small fraction of the neurons within their large axonal arborisation (Martin et al., '83; Somogyi et al., '83b), clutch cells, with their compact axonal field, seem to provide input to a much higher proportion of neurones within their axonal field. In this respect they are quite similar to LGN afferents that terminate in the same layer.

Possible transmitter of clutch cells

Most boutons forming type II contacts in the cat visual cortex have been shown to be immunoreactive for GAD (Freund et al., '83) and GABA (Somogyi and Hodgson, '85).

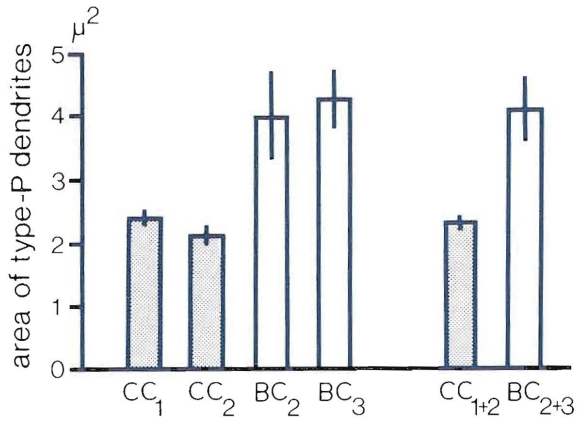

Fig. 18. Comparison of the area (mean ± S.E.M.) of type P profiles that received synapses from clutch cells 1 and 2 (CC_1, n = 55, CC_2, n = 29) in layer IV with those that received synapses from large basket cells (BC_2, n = 24, BC_3, n = 12) in layer III. Basket cell data is based on new measurements from material published earlier (Somogyi et al., '83). Clutch cells make synapses with significantly smaller dendrites ($P < .01$, F test) than do large basket cells.

Fig. 19. Comparison of dendrites postsynaptic to clutch cell No. 1 (filled triangles, line P_1; filled circles, line S_1) and clutch cell No. 2 (open triangles, line P_2; circles, line S_2). Measurements were taken from electron micrographs photographed at the site where the HRP-filled boutons made synaptic contacts with them. Linear regression lines were used as centres of gravity to show that both cells contact similar populations of dendrites. Type P dendrites are more homogenous than type S dendrites and probably originate from pyramidal and spiny stellate cells. Type S dendrites probably belong to aspiny and sparsely spiny nonpyramidal neurons. The dendrites of clutch cell 1 (filled squares, D_{CC1}) are similar to type S dendrites.

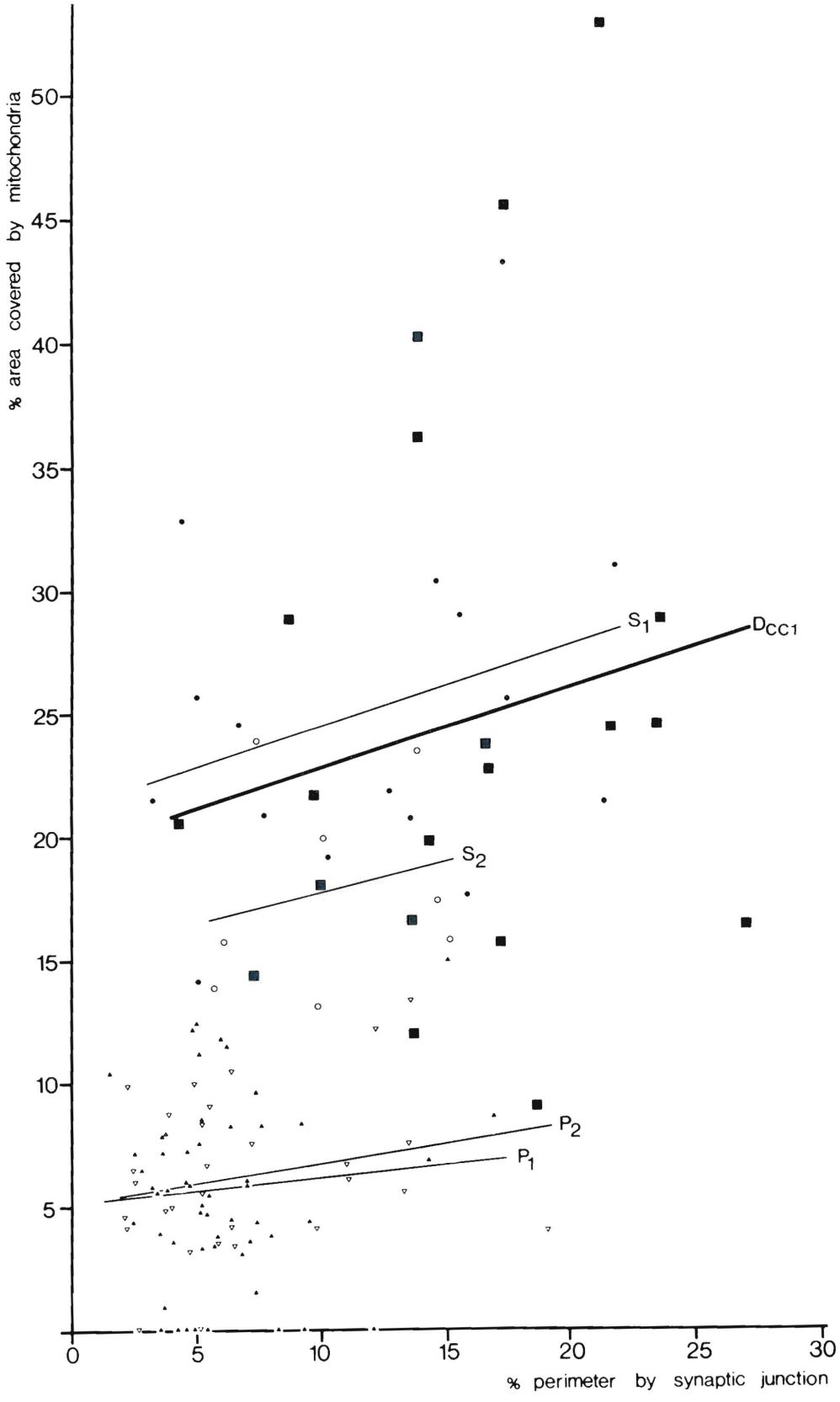
% area covered by mitochondria
50
45
40
35
30
25
20
15
10
5
0
5
10
15
20
25
30
% perimeter by synaptic junction
S1
DCC1
S2
P2
P1

Figure 19

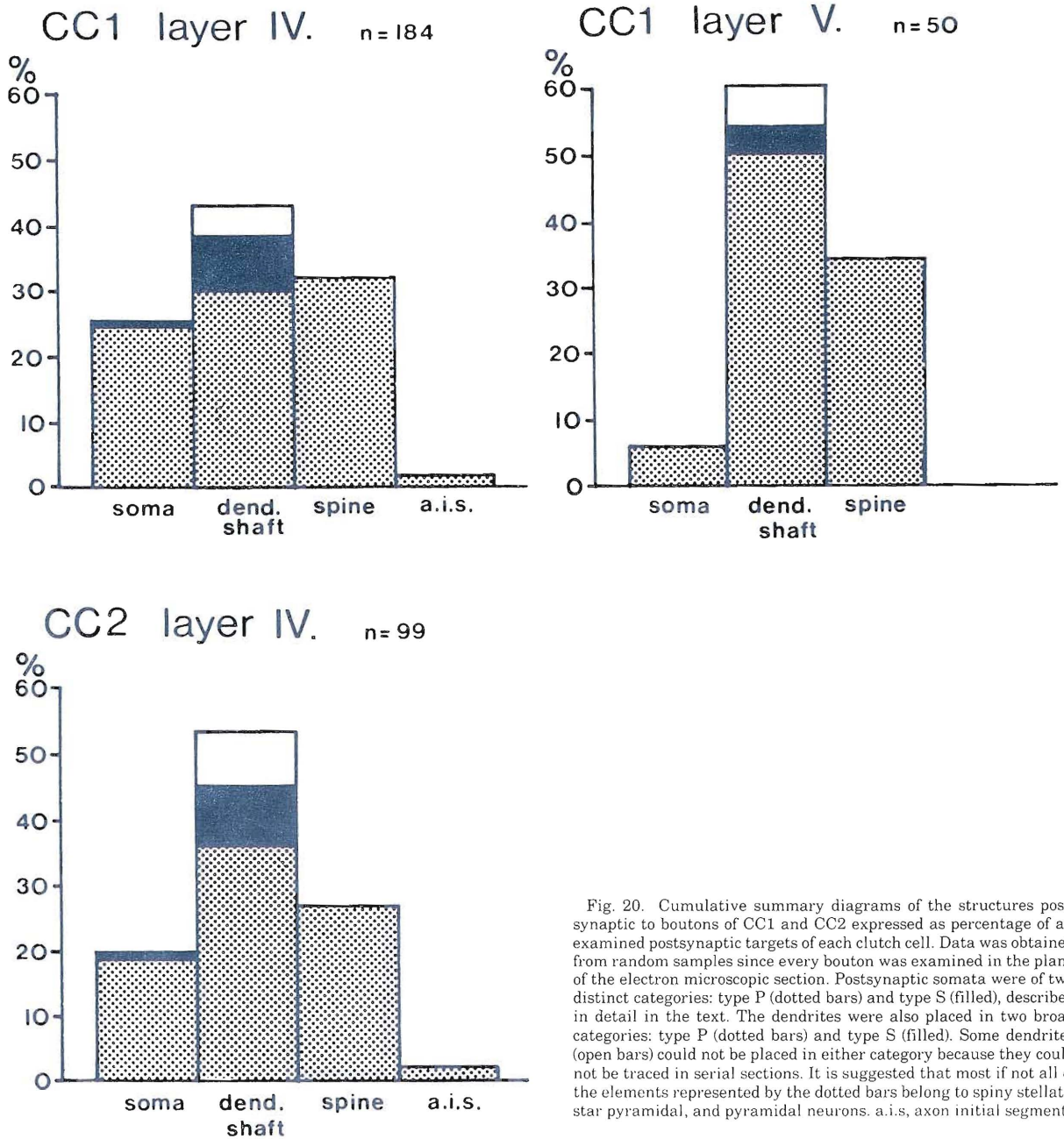

Fig. 20. Cumulative summary diagrams of the structures postsynaptic to boutons of CC1 and CC2 expressed as percentage of all examined postsynaptic targets of each clutch cell. Data was obtained from random samples since every bouton was examined in the plane of the electron microscopic section. Postsynaptic somata were of two distinct categories: type P (dotted bars) and type S (filled), described in detail in the text. The dendrites were also placed in two broad categories: type P (dotted bars) and type S (filled). Some dendrites (open bars) could not be placed in either category because they could not be traced in serial sections. It is suggested that most if not all of the elements represented by the dotted bars belong to spiny stellate, star pyramidal, and pyramidal neurons. a.i.s, axon initial segment

Furthermore most boutons on the somata of neurons in layer IV, where clutch cells also terminate, were immunoreactive for GABA in the present study. Although direct evidence on the transmitters of identified clutch cells is not yet available, the above circumstantial evidence strongly suggests that they are GABAergic and presumably inhibitory (Curtis and Johnston, '74; Krnjević, '74). While admittedly more direct evidence is needed for this assumption, it is worth considering the possible effect of a clutch-cell-mediated inhibition in the light of the distribution of its synaptic terminals.

Consequences of somatic inhibition

One major target of clutch cells is the somatic region of spiny cells. Theoretical considerations (Blomfield, '74) predicted a divisionlike change in the firing rate of the neurone if inhibitory conductances on the soma were large, in contrast to the subtractive changes predicted as a result of

inhibition on distal dendrites (Blomfield, '74; Jack et al., '75). In the visual cortex, there is evidence that the inhibition underlying orientation selectivity (Rose, '77; Morrone et al., '82) and direction selectivity (Dean et al., '80) involves divisive changes in firing. Thus the generation of these properties is likely to involve somatic inhibition. Unfortunately, since the neurons in the above studies could not be identified we cannot yet establish if clutch cells, or large basket cells (which also give perisomatic synapses—Somogyi et al., '83b), were involved in the inhibition. As yet no attempt has been made to simulate a situation where simultaneous dendritic and somatic inhibition are produced by the same cells, but nonlinearities could be expected even in such an arrangement (Blomfield, '74).

Relationship of clutch cells and LGN axons

Ordinal position. Response latencies to electrical stimulation showed for CC1 that it was monosynaptically activated by Y afferents (Martin et al., '83). The units recorded during the injection of CC2 and CC3 also showed monosynaptic latencies and Y input. One of the main inputs of layer IV in area 18 comes from Y afferents, and the dendritic arbor of CC3, which was restricted to layer IV, provides a structural basis for the input. Most if not all cells in layer IV of the striate cortex are monosynaptically driven by LGN afferents (Toyama et al., '73; Henry et al., '79; Bullier and Henry, '79; Ferster and Lindström, '83; Martin and Whitteridge, '84). The characteristics of the large boutons terminating on CC1 and CC3 also suggest monosynaptic LGN input to clutch cells. Such large boutons densely filled with round vesicles and establishing type I synaptic contacts with GABA-immunoreactive somata in layer IV, of both area 18 and 17, were recently shown to originate from physiologically identified X and Y LGN axons (Freund et al., in press). LGN fibers rarely form axosomatic synapses and all of these seem to be on a particular class of neuron in layer IV (Garey and Powell, '71; Davis and Sterling, '79; Hornung and Garey, '81; Hamos et al., '83). The fine structural features, size, and somatic input of clutch cells studied here and in neurons shown in the above studies are in good agreement. A recent combined intracellular HRP/EM study (McGuire et al., '84) suggests that the clutch cell might also get an input on its distal dendrites from layer VI pyramids. This input is less direct than the LGN input and may only be facilitatory in its effect.

Bouton and synapse distribution. The laminar bias of clutch cell terminals suggests a relationship with the LGN afferent projection to layer IV. The clutch cells do not respect the IVA/B border and could interact with cells receiving either X or Y input. Although there is some bias in the input to the A and B laminae of layer IV, the strict segregation of X and Y axon terminals suggested by earlier studies (Ferster and LeVay, '78; Gilbert and Wiesel, '79) does not seem to be confirmed by recent intra-axonal injection studies (Humphrey and Ulrich, '84; Martin, '84). It is interesting to compare the axon of CC1 that was activated by Y afferents with the Y axon arbor published by Gilbert and Wiesel ('83, their Fig. 12). The Y axon had two clumps of terminals each probably forming part of an ocular dominance column and each about the size of the total arbor of the clutch cell shown here (300 × 500 μm). The clustering of boutons within one patch of the Y axon is strikingly similar to that seen for the clutch cell boutons: both have a 100-μm-wide gap between bouton clusters, as indicated by Gilbert and Wiesel ('83).

The convergence of clutch cell and LGN axonal systems at the level of the single cell, or parts of a cell such as dendrites and spines, is almost inevitable if we take into account that most cells in layer IV receive monosynaptic LGN input and most neurones in the axonal field of clutch cells are contacted by its terminals. In this respect the clutch cell terminals establishing synapses with dendritic shafts and spines deserve attention since these are the elements at which most geniculate axons terminate (Garey and Powell, '71; Davis and Sterling, '79; Hornung and Garey, '81); thus there may be a close relationship between the two sets of terminals.

The dendritic field of clutch cells is within the field of its axon terminals; thus, from the retinotopic and columnar organisation of the cortex it could be expected that clutch cells receive input from the same set of afferents as some of the neurones they contact. Analysis of the distribution of neurones that receive somatic input from the clutch cells confirms that this is the case. This implies that there may be simultaneous activation and inhibition of neurones, even when optimal stimuli are applied. This apparent paradox has in fact been demonstrated by physiological experiments showing that inhibitory and excitatory postsynaptic potentials can be elicited from the same region of the receptive field (Creutzfeldt and Ito, '68) and are also present when optimal stimuli are used (Creutzfeldt et al., '74). In this situation the spatial position of the receptive fields providing the excitatory input relative to receptive fields of the inhibitory input will be important in determining the resultant functional properties of the cell. In a recent model, orientation selectivity was explained on the basis of partially overlapping excitatory and inhibitory fields with slightly displaced centers (Heggelund and Moors, '83). It is worth noting that the dendritic field and the soma of CC1 was asymmetrically placed within its axonal field. If all clutch cells have a similar arrangement, this could lead to inhibition of neurons whose receptive field positions on average are slightly displaced relative to those of a pool of clutch cells having the elongated axonal fields asymmetrically placed to their dendritic field. Such wiring might also come about as a consequence of the jitter in the receptive fields of successive cells in a radial column (Hubel and Wiesel, '62; Albus, '75).

Complex cell to simple cell inhibition

One of the clutch cells was clearly identified as having a C- or complex-type receptive field. These cells are relatively rare in layer IV; the simple or S cells form the great majority of cells in layer IV. This makes it likely that the clutch cell contacted simple cells. Such a complex-to-simple-cell inhibitory pathway has been predicted on the basis of experiments showing that simple cells are inhibited by noise stimuli to which the complex cells respond selectively (Hammond and MacKay, '81; Morrone et al., '82). Although we did not test the particular cell with noise stimuli, this cell could be one source of inhibition underlying the mechanism.

CONCLUSIONS

If we wish to understand the cortical circuitry then we have to identify the relationships between the structure of the component parts and their functional properties. Layer

IV is the obvious starting point for this analysis because it is the major recipient zone of the thalamic input. Although the present methods are necessarily time consuming and the data as yet fragmented, they are providing new details of the microcircuitry in layer IV (McGuire et al., '84; Martin, '84; Somogyi et al., '83b). A picture is emerging of different cell types providing input not only to particular types of neuron, but also showing preferences for particular regions of the postsynaptic cell. It is only identifying the rules governing these complex patterns of connectivity that we will be able to derive realistic models of cortical function.

ACKNOWLEDGMENTS

We are grateful to Mrs. Klára Boczkó and Mr. John Anderson for excellent technical assistance, to Mrs. Judy Gotch for typing the manuscript, and to Dr. J. Somogyi for his help in the computing. This work was supported by the Medical Research Council, U.K., the Hungarian Academy of Sciences, the International Cultural Institute, Budapest, the National Health and Medical Research Council of Australia, and the C. and V. Ramaciotti Foundation, Australia.

LITERATURE CITED

Adams, J.C. (1981) Heavy metal intensification of DAB-based HRP reaction product. J. Histochem. Cytochem. *29:*775.

Albus, K. (1975) A quantitative study of the projection area of the central and the paracentral visual field in area 17 of the cat. I. The precision of the topography. Exp. Brain Res. *24:*159–179.

Benevento, L.A., O.D. Creutzfeldt, and U. Kuhnt (1972) Significance of intracortical inhibition in the visual cortex. Nature *238:*124–126.

Bishop, P.O., J.S. Coombs, and G.H. Henry (1971) Interaction effects of visual contours on the discharge frequency of simple striate neurons. J. Physiol. (Lond.) *219:*659–687.

Blakemore, C., and E.A. Tobin (1972) Lateral inhibition between orientation detectors in the cat's visual cortex. Exp. Brain Res. *15:*439–440.

Blomfield, S. (1974) Arithmetical operations performed by nerve cells. Brain Res. *69:*115–124.

Bullier, J., and G.H. Henry (1979) Laminar distribution of first-order neurons and afferent terminals in cat striate cortex. J. Neurophysiol. *42:*1271–1281.

Burr, D., C. Morrone, and L. Maffei (1981) Intracortical inhibition prevents simple cells from responding to textured visual patterns. Exp. Brain Res. *43:*455–458.

Creutzfeldt, O.D., and M. Ito (1968) Functional synaptic organization of primary visual cortex neurones in the cat. Exp. Brain Res. *6:*324–352.

Creutzfeldt, O.D., U. Kuhnt, and L.A. Benevento (1974) An intracellular analysis of visual cortical neurones to moving stimuli: Responses in a co-operative neuronal network. Exp. Brain Res. *21:*251–274.

Curtis, D.R., and G.A.R. Johnston (1974) Amino acid transmitters in the mammalian central nervous system. Ergeb. Physiol. *69:*97–188.

Davis, T.L., and P. Sterling (1979) Microcircuitry of cat visual cortex: Classification of neurons in layer IV of area 17, and identification of the patterns of lateral geniculate input. J. Comp. Neurol. *188:*599–627.

Dean, A.F., R.F. Hess, and D.J. Tolhurst (1980) Divisive inhibition involved in directional selectivity. J. Physiol. (Lond.) *308:*84–85P.

DeFelipe, J., and A. Fairén (1982) A type of basket cell in superficial layers of the cat visual cortex. A Golgi-electron microscope study. Brain Res. *244:*9–16.

Eccles, J.C. (1964) The Physiology of Synapses. Berlin: Springer-Verlag.

Emson, P.C., and O. Lindvall (1979) Distribution of putative neurotransmitters in the neocortex. Neuroscience *4:*1–30.

Fairén, A., and F. Valverde (1980) A specialized type of neuron in the visual cortex of cat: A Golgi and electron microscope study of chandelier cells. J. Comp. Neurol. *194:*761–779.

Ferster, D., and S. LeVay (1978) The axonal arborizations of lateral geniculate neurons in the striate cortex of the cat. J. Comp. Neurol. *182:*923–944.

Ferster, D., and S. Lindström (1983) An intracellular analysis of geniculocortical connectivity in area 17 of the cat. J. Physiol. (Lond.) *342:*181–217.

Freund, T.F., K.A.C. Martin, A.D. Smith, and P. Somogyi (1983) Glutamate decarboxylase-immunoreactive terminals of Golgi-impregnated axo-axonic cells and of presumed basket cells in synaptic contact with pyramidal cells of the cat's visual cortex. J. Comp. Neurol. *221:*263–278.

Freund, T.F., K.A.C. Martin, P. Somogyi, and D. Whitteridge. Innervation of cat visual areas 17 and 18 by physiologically identified X- and Y-type thalamic afferents. II. Identification of postsynaptic targets by GABA immunocytochemistry and Golgi impregnation. J. Comp. Neurol. (In press).

Garey, L.J., and T.P.S. Powell (1971) An experimental study of the termination of the lateral geniculocortical pathways in the cat and monkey. Proc. R. Soc. Lond. [Biol.] *179:*41–63.

Gilbert, C.D., and T.N. Wiesel (1979) Morphology and intracortical projections of functionally characterised neurones in the cat visual cortex. Nature *280:*120–125.

Gilbert, C.D., and T.N. Wiesel (1983) Clustered intrinsic connections in cat visual cortex. J. Neurosci. *3:*1116–1133.

Hammond, P., and D.M. MacKay (1981) Modulatory influences of moving textured backgrounds on responsiveness of simple cells in feline striate cortex. J. Physiol. (Lond.) *319:*431–442.

Hamos, J.E., T.L. Davis, and P. Sterling (1983) Four types of neuron in layer IVab of cat cortical area 17 accumulate ^{3}H-GABA. J. Comp. Neurol. *217:*449–457.

Hanker, J.S., P.E. Yates, C.B. Metz, and A. Rustioni (1977) A new specific sensitive and non-carcinogenic agent for the demonstration of horseradish peroxidase. Histochem. J. *9:*789–792.

Heggelund, P., and J. Moors (1983) Orientation selectivity and the spatial distribution of enhancement and suppression in receptive fields of cat striate cortex cells. Exp. Brain Res. *52:*235–247.

Henry, G.H., A.R. Harvey, and J.S. Lund (1979) The afferent connections and laminar distribution of cells in the cat striate cortex. J. Comp. Neurol. *187:*725–744.

Hodgson, A.J., B. Penke, A. Erdei, I.W. Chubb, and P. Somogyi (1985) Antiserum to γ-aminobutyric acid: I. Production and characterization using a new model system. J. Histochem. Cytochem. *33:*229–239.

Hoffmann, K.P., and J. Stone (1971) Conduction velocity of afferents to cat visual cortex: A correlation with cortical receptive field properties. Brain Res. *32:*460–466.

Hornung, J.P., and L.J. Garey (1981) The thalamic projection to cat visual cortex: Ultrastructure of neurons identified by Golgi impregnation or retrograde horseradish peroxidase transport. Neuroscience *6:*1053–1068.

Hubel, D.H., and T.N. Wiesel (1962) Receptive fields, binocular interaction and functional architecture in the cat's visual cortex. J. Physiol. (Lond.) *160:*106–154.

Humphrey, A.L., and D.J. Ulrich (1984) The laminar projections of X- and Y-cell axons in layer IV of cat area 17 reflect the cells' locations within the depths of the A-laminae of the LGN. Soc. Neurosci. Abstr. *10:*520.

Jack, J.J.B., D. Noble, and R.W. Tsien (1975) Electric current flow in excitable cells. Oxford, Oxford University Press, pp. 197–222.

Kisvárday, Z.F., K.A.C. Martin, P. Somogyi, and D. Whitteridge (1983) The physiology, morphology and synaptology of basket cells in the cat's visual cortex. J. Physiol. (Lond.)*334:*21–22P.

Krnjević, K. (1974) Chemical nature of synaptic transmission in vertebrates. Physiol. Rev. *54:*418–540.

LeVay, S. (1973) Synaptic patterns in the visual cortex of the cat and monkey. Electron microscopy of Golgi preparations. J. Comp. Neurol. *150:*53–85.

Lund, J.S. (1973) Organisation of neurons in the visual cortex, area 17, of the monkey (Macaca mulatta). J. Comp. Neurol. *147:*455–496.

Lund, J.S. (1984) Spiny stellate neurons. In A. Peters and E.G. Jones (eds): Cerebral Cortex. New York: Plenum Press, Vol. 1, pp. 255–308.

Lund, J.S, G.H. Henry, C.L. MacQueen, and A.R. Harvey (1979) Anatomical organization of the primary visual cortex (Area 17) of the cat. A comparison with area 17 of the macaque monkey. J. Comp. Neurol. *184:*599–618.

Martin, K.A.C. (1984) Neuronal circuits in cat striate cortex. In E.G. Jones and A. Peters (eds): Cerebral Cortex. New York: Plenum Press, Vol. 2, pp. 241–284.

Martin, K.A.C., P. Somogyi, and D. Whitteridge (1983) Physiological and morphological properties of identified basket cells in the cat's visual cortex. Exp. Brain Res. *50:*193–200.

Martin, K.A.C., and D. Whitteridge (1984) Form, function, and intracortical projections of spiny neurones in the striate visual cortex of the cat. J. Physiol. (Lond.) *353:*463–504.

Mates, S.L., and J.S. Lund (1983) Neuronal composition and development in lamina 4C of monkey striate cortex. J. Comp. Neurol. *221:*60–90.

McGuire, B.A, J.-P. Hornung, C.D. Gilbert, and T.N. Wiesel (1984) Patterns of synaptic input to layer 4 of cat striate cortex. J. Neurosci. *4:*3021–3033.

Meyer, G. (1983) Axonal patterns and topography of short-axon neurons in visual areas 17, 18, and 19 of the cat. J. Comp. Neurol. *220:*405–438.

Morrone, M.C., D.C. Burr, and I. Maffei (1982) Functional implications of cross-orientation inhibition of cortical visual cells. I. Neurophysiological evidence. Proc. R. Soc. Lond. [Biol.] *216:*335–354.

O'Leary, J.L. (1941) Structure of area striata of cat. J. Comp. Neurol. *75:*131–164.

Palay, S.L., C. Sotelo, A. Peters, and P.M. Orkand (1968) The axon hillock and the initial segment. J. Cell Biol. *38:*193–201.

Perry, V.H., and R. Linden (1982) Evidence for dendritic competition in the developing retina. Nature *297:*683–685.

Peters, A., and J. Regidor (1981) A reassessment of the forms of nonpyramidal neurons in area 17 of cat visual cortex. J. Comp. Neurol. *203:*685–716.

Peters, A., and R.L. Saint Marie (1984) Smooth and sparsely spinous nonpyramidal cells forming local axonal plexuses. In A. Peters and E.G. Jones (eds): Cerebral Cortex. New York: Plenum Press, Vol. 1, pp. 419–445.

Ramón y Cajal, S. (1899) Estudios sobre la corteza cerebral humana. Corteza visual. Rev. Trim. Microgr. *4:*1–63.

Ribak, C.E. (1978) Aspinous and sparsely-spinous stellate neurons in the visual cortex of rats contain glutamic acid decarboxylase. J. Neurocytol. *7:*461–478.

Rose, D. (1977) On the arithmetic operations performed by inhibitory synapses onto the neuronal soma. Exp. Brain Res. *28:*221–223.

Sillito, A.M. (1975) The contribution of inhibitory mechanisms to the receptive field properties of neurons in the striate cortex of the cat. J. Physiol. (Lond.) *250:*305–329.

Sillito, A.M. (1977) Inhibitory processes underlying the directional specificity of simple, complex and hypercomplex cells in the cat's visual cortex. J. Physiol. (Lond.) *271:*699–720.

Sillito, A.M. (1979) Inhibitory mechanisms influencing complex cell orientation selectivity and their modification at high resting discharge levels. J. Physiol. (Lond.) *289:*33–53.

Somogyi, P., A.J. Hodgson, and A.D. Smith (1979) An approach to tracing neuron networks in the cerebral cortex and basal ganglia. Combination of Golgi-staining, retrograde transport of horseradish peroxidase and anterograde degeneration of synaptic boutons in the same material. Neuroscience *4:*1805–1852.

Somogyi, P., T.F. Freund, J.-Y. Wu, and A.D. Smith (1983a) The section-Golgi impregnation procedure. 2. Immunocytochemical demonstration of glutamate decarboxylase in Golgi-impregnated neurons and in their afferent synaptic boutons in the visual cortex of the cat. Neuroscience *9:*475–490.

Somogyi, P., Z.F. Kisvárday, K.A.C. Martin, and D. Whitteridge (1983b) Synaptic connections of morphologically identified and physiologically characterized large basket cells in the striate cortex of cat. Neuroscience *10:*261–294.

Somogyi, P., A.J. Hodgson, A.D. Smith, M.G. Nunzi, A. Gorio, and J.-Y. Wu (1984) Different populations of GABA-ergic neurons in the visual cortex and hippocampus of cat contain somatostatin- or cholecystokinin-immunoreactive material. J. Neurosci. *4:*2590–2603.

Somogyi, P., A.J. Hodgson, I.W. Chubb, B. Penke, and A. Erdei (1985) Antiserum to γ-aminobutyric acid: II. Immunocytochemical application to the central nervous system. J. Histochem. Cytochem. *33:*240–248.

Somogyi, P., and A.J. Hodgson (1985) Antiserum to γ-aminobutyric acid: III. Demonstration of GABA in Golgi-impregnated neurons and in conventional electron microscopic sections of cat striate cortex. J. Histochem. Cytochem. *33:*249–257.

Sternberger, L.A., P.H. Hardy Jr, J.J. Cuculis, and H.G. Meyer (1970) The unlabeled antibody enzyme method of immunohistochemistry. Preparation and properties of soluble antigen-antibody complex (horseradish peroxidase-antihorseradish peroxidase) and its use in identification of spirochetes. J. Histochem. Cytochem. *18:*315–333.

Szentágothai, J. (1973) Synaptology of the visual cortex. In R. Jung (ed): Handbook of Sensory Physiology. New York: Springer, VII/3B, pp. 270–321.

Tolhurst, D.J., and I.D. Thompson (1982) Organizations of neurons preferring similar spatial frequencies in cat striate cortex. Exp. Brain Res. *48:*217–227.

Toyama, K., K. Maekawa, and T. Takeda (1977) Convergence of retinal inputs onto visual cortical cells. I. A study of the cells monosynaptically excited from the lateral geniculate body. Brain Res. *137:*207–220.

Tsumoto, T., W. Eckart, and O.D. Creutzfeldt (1979) Modification of orientation sensitivity of cat visual cortex neurons by removal of GABA-mediated inhibition. Exp. Brain Res. *34:*351–363.

Valverde, F. (1971) Short axon neuronal subsytems in the visual cortex of the monkey. Int. J. Neurosci. *1:*181–197.

Valverde, F. (1978) The organisation of area 18 in the monkey. A Golgi study. Anat. Embryol. (Berl.) *154:*305–334.

Zsuppan, F. (1984) A new approach to merging neuronal tree segments traced from serial sections. J. Neurosci. Methods *10:*199–204.